

Frustrated Lewis Pair Modification by 1,1-Carboboration: Disclosure of a Phosphine Oxide Triggered Nitrogen Monoxide Addition to an Intramolecular P/B Frustrated Lewis Pair

René Liedtke,[†] Felix Scheidt,[†] Jinjun Ren,[‡] Birgitta Schirmer,[†] Allan Jay P. Cardenas,[§] Constantin G. Daniliuc,[†] Hellmut Eckert,^{*,‡} Timothy H. Warren,^{*,§} Stefan Grimme,^{*,||} Gerald Kehr,[†] and Gerhard Erker^{*,†}

[†]Organisch-Chemisches Institut, Universität Münster, Corrensstrasse 40, Münster 48149, Germany

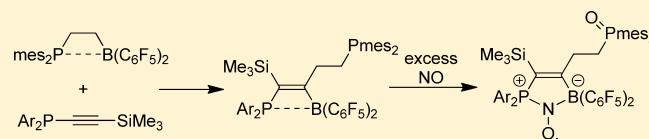
[‡]Institut für Physikalische Chemie, Universität Münster, Corrensstrasse 30, Münster 48149, Germany

[§]Department of Chemistry, Georgetown University, 37th and O Streets NW, Washington, DC 20057-1227, United States

^{||}Mulliken Center for Theoretical Chemistry, Institut für Physikalische und Theoretische Chemie, Universität Bonn, Beringstrasse 4, Bonn 53115, Germany

S Supporting Information

ABSTRACT: The vicinal frustrated Lewis pair (FLP) $\text{mes}_2\text{P}-\text{CH}_2\text{CH}_2-\text{B}(\text{C}_6\text{F}_5)_2$ (**3**) reacts with phenyl(trimethylsilyl)acetylene by 1,1-carboboration to give the extended C_3 -bridged FLP **6** featuring a substituted vinylborane subunit. The FLP **6** actively cleaves dihydrogen. The FLP **3** also undergoes a 1,1-carboboration reaction with diphenylphosphino-(trimethylsilyl)acetylene to give the P/B/P FLP **11** that features a central unsaturated four-membered heterocyclic P/B FLP and a pendant $\text{CH}_2\text{CH}_2-\text{Pmes}_2$ functional group. Compound **11** reacts with nitric oxide (NO) by oxidation of the pendant Pmes_2 unit to the $\text{P}(\text{O})\text{mes}_2$ phosphine oxide and N,N-addition of the P/B FLP unit to NO to yield the persistent P/B/PO FLPNO aminoxyl radical **14**. This reaction is initiated by $\text{P}(\text{O})\text{mes}_2$ formation and opening of the central $\text{Ph}_2\text{P}\cdots\text{B}(\text{C}_6\text{F}_5)_2$ linkage triggered by the pendant $\text{CH}_2\text{CH}_2-\text{P}(\text{O})\text{mes}_2$ group.



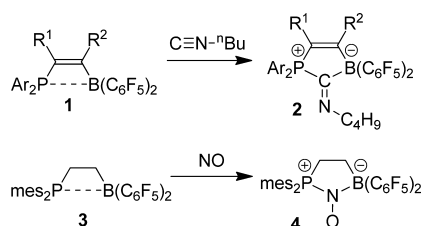
INTRODUCTION

Intramolecular frustrated Lewis pairs (FLPs) can undergo quite some remarkable reactions.¹ Some of such main group element Lewis acid/Lewis base combinations show a transition-metal-reminiscent coordination behavior with selected small-molecule ligands.² Typical examples are the formation of the isonitrile-bridged addition products **2** derived from a small series of the unsaturated intramolecular vicinal P/B FLPs **1**³ (see Scheme 1). Binding of the isonitrile donor to the boron Lewis acid of **1** in these cases is strongly amended by a backbonding interaction from the adjacent phosphane donor to the isonitrile π^* orbital, resulting in an overall bonding situation that is remotely reminiscent of the bonding/backbonding combination of ligands at single transition-metal centers as it is commonly

described by the Dewar–Chatt–Duncanson model.⁴ Of course, in contrast to the d-metal situation, the donor and acceptor functions are separated from each other in a FLP and residing on different atoms. A similar situation has been encountered upon treatment of the saturated ethylene-bridged vicinal P/B FLP **3**⁵ with nitric oxide (NO). In this case, the cooperative addition of the boron acceptor and the phosphane donor to the nitrogen atom of nitrogen monoxide has resulted in the formation of the persistent heterocyclic FLPNO radical **4** (see Scheme 1).^{6c}

Various substituted derivatives of **3** have been shown to also undergo this reaction under mild conditions to yield the respective substituted FLPNO systems.⁶ Examples of the compound **1** so far have been resistant to NO addition. However, we have now prepared a variety of analogues of **1** featuring an additional pendant Pmes_2 group at the periphery of the FLP core. In contrast to **1**, these new systems showed a remarkable reactivity toward nitrogen monoxide as will be described and discussed in this account. Moreover, we found out that the 1,1-carboboration reaction turned out to be an ideally suited tool for the modification and functionalization of FLPs.

Scheme 1



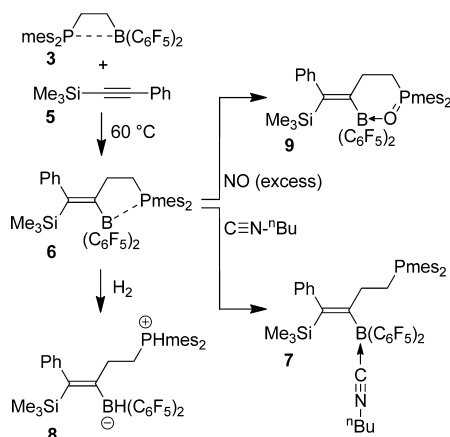
Received: March 27, 2014

Published: May 21, 2014

RESULTS AND DISCUSSION

Frustrated Lewis Pair Modification by the 1,1-Carboboration Reaction. Silyl substituents have long been known to serve as good migrating groups in classical 1,1-carboboration reactions (“Wrackmeyer reaction”).⁷ We and others have more recently shown which the use of strongly electrophilic R-B(C₆F₅)₂ boranes greatly facilitated 1,1-carboboration reactions, extending their application potential significantly.^{3,8–12} Therefore, we treated the P/B FLP **3** (bearing the strongly electrophilic B(C₆F₅)₂ functionality) with trimethylsilylphenylacetylene (**5**). Not unexpectedly, these two reagents underwent a clean 1,1-carboboration reaction at 60 °C to give the extended and alkylidene functionalized new FLP **6** in good yield (see Scheme 2). The

Scheme 2



NMR characterization revealed that **6** features a B–P interaction as expected. This has become evident by the typical NMR chemical shifts of the pair of core heteronuclei (³¹P: δ 26.5; ¹¹B: δ 4.7). Consistently, the ¹⁹F NMR spectrum of **6** shows three signals (*o*, *p*, *m*) of the pair of symmetry-equivalent C₆F₅ groups at boron with a relatively small Δδ¹⁹F(*m*, *p*) separation of 7.2 ppm (for further details see the Experimental Section and the Supporting Information). The ring-expanded C₃-bridged P/B FLP **6** reacted rapidly with one molar equivalent of *n*-butylisocyanide¹³ to give the adduct **7** (78% isolated). It was characterized by C,H,N elemental analysis, by spectroscopy and by X-ray diffraction (single crystals were obtained from pentane at –40 °C).

The X-ray crystal structure analysis of compound **7** (see Figure 1) shows that the (Me₃Si)PhC=C vinylidene isomer of **5**¹⁴ has formally become inserted into the [B]–CH₂ linkage of **3**. Of course, this has taken place by the typical mechanistic 1,1-carboboration sequence, probably with the SiMe₃ substituent serving as one migrating group^{11a,15} and the CH₂CH₂–Pmes₂ moiety as the other. This has resulted in the formation of the C₃-bridge between phosphorus and boron including the Me₃Si/Ph-substituted exomethylene group at its α position. The isocyanide donor has added to the boron Lewis acid, thereby cleaving the B–P bond of the starting material **6**. Consequently, the boron atom shows a pseudotetrahedral coordination geometry, and the phosphorus atom shows a trigonal-pyramidal coordination geometry.

In solution, compound **7** shows NMR signals at δ –18.9 (¹⁰B), δ –21.6 (³¹P), and δ –11.4 (²⁹Si). It features ¹H NMR resonances of the CH₂CH₂ unit at δ 2.50 and δ 2.14 and ¹³C

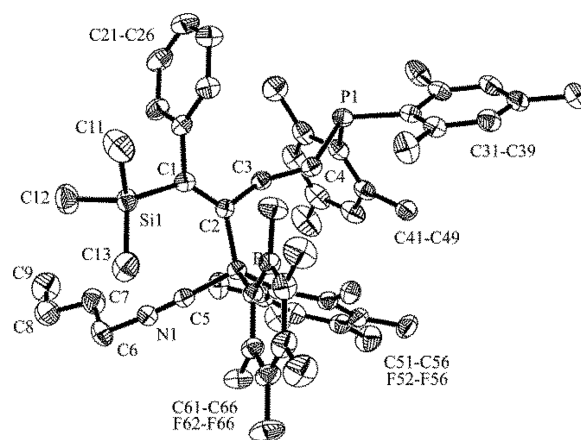


Figure 1. Molecular structure of the FLP–isonitrile adduct **7** (thermal ellipsoids are shown with 30% probability). Selected bond lengths (Å) and angles (deg): P1–C4:1.861(3), C4–C3:1.537(4), C3–C2:1.518(4), C2–C1:1.362(4), C2–B1:1.639(4), B1–C5:1.612(5), C5–N1:1.136(4), C3–C2–C1:119.0(2), C3–C2–B1:115.2(2), C1–C2–B1:125.8(3), C21–C1–Si1:109.0(2), C2–B1–C5:104.9(2), B1–C5–N1:177.0(3), C5–N1–C6:173.6(3), P1–C4–C3–C2:161.56, ΣP^{CCC} = 313.9.

NMR signals of the substituted exomethylene group at δ 157.3 (=C[B]) and δ 149.4 (=C[Si]), respectively.

The new C₃-bridged P/B FLP **6** reacts with dihydrogen under mild reaction conditions.¹⁶ Treatment of in situ generated **6** with H₂ (rt, 1.5 bar, overnight) resulted in heterolytic cleavage of the dihydrogen molecule with formation of the C₃-bridged phosphonium/hydridoborate product **8** (49% isolated). The composition of **8** was confirmed by X-ray diffraction (see the Supporting Information). Compound **8** shows typical doublets in the ¹¹B (δ –19.6, ¹J_{BH} ~ 85 Hz) and ³¹P (δ –11.6, ¹J_{PH} = 468 Hz) NMR spectra with corresponding ¹H NMR resonances at δ 3.51 (br, [B]H) and δ 6.73 (dt, ¹J_{PH} = 468 Hz, ³J_{HH} = 7.0 Hz, [P]H), respectively (for further details and the depicted NMR spectra see the Supporting Information).

Compound **6** reacts with nitric oxide, but it apparently shows only the typical reaction behavior of the phosphane to nitrogen monoxide. It is well known that many phosphanes react with NO to give the corresponding phosphine oxides with concomitant formation of N₂O.¹⁷ Compound **6** is no exception. We treated the FLP **6** with excess NO (1.5 bar) for 2 h at room temperature (rt) and isolated the phosphine oxide **9** in 61% yield. The X-ray crystal structure analysis revealed that the Pmes₂ moiety had been converted to P(O)mes₂ and the newly introduced oxygen atom had coordinated to the boron atom forming a [P]=O Lewis base/RB(C₆F₅)₂ Lewis acid adduct. The resulting six-membered heterocycle is nonplanar (θ P1–C1–C2–C3: 73.9(2)°). The sp²-carbon atom C3 is part of the exocyclic C=C double bond (see Figure 2). Both the phosphorus and the boron atoms show pseudotetrahedral coordination geometries (ΣP^{CCC} = 333.6°; ΣB^{CCC} = 342.6°).

In solution, compound **9** shows ¹H NMR signals of the CH₂CH₂ moiety at δ 2.65 and 2.76 with corresponding ¹³C NMR resonances at δ 29.0 (²J_{PC} = 6.3 Hz) and δ 29.7 (¹J_{PC} = 57.0 Hz), respectively. The Ph[Si]C=C ¹³C NMR signals occur at δ 160.1 (C[B]) and δ 144.2 (C[Si]), respectively, and we have monitored the core heteroatom magnetic resonance signals at δ 0.0 (¹¹B) and δ 62.4 (³¹P), respectively (²⁹Si: δ –10.4).

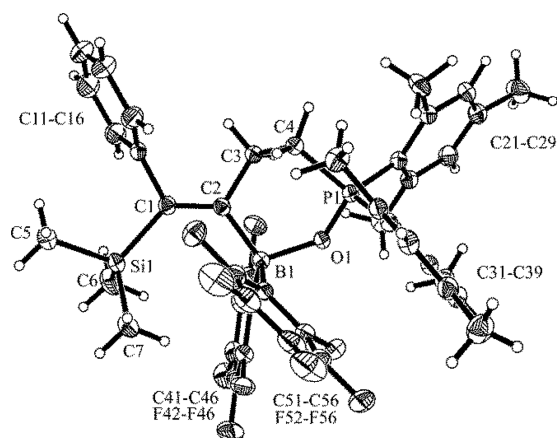
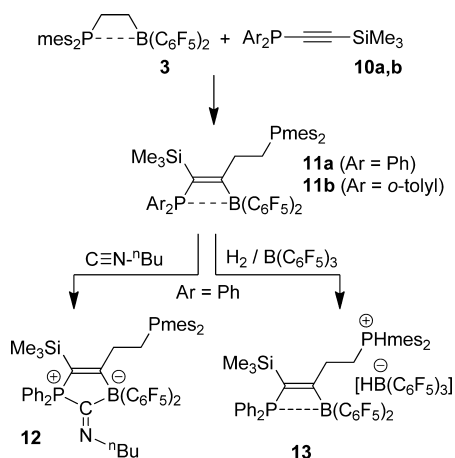


Figure 2. Molecular structure of compound **9** (thermal ellipsoids are shown with 30% probability). Selected bond lengths (Å) and angles (deg): P1–O1:1.544(1), B1–O1:1.591(2), B1–C2:1.637(3), C1–C2:1.353(3), C3–C2:1.520(3), C3–C4:1.535(3), C4–P1:1.801(2), C4–P1–O1:103.5(1), P1–O1–B1:124.7(1), O1–B1–C2:107.3(2), B1–C2–C1:128.1(2), Si1–C1–C11:110.3(1), C1–C2–C3:119.2(2), C4–C3–C2:111.6(2).

Formation and Characterization of the New P/B/P Frustrated Lewis Pairs. We treated diphenylphosphino-(trimethylsilyl)acetylene (**10a**) with the ethylene-bridged FLP **3**. It apparently formed a B/P Lewis acid/base adduct upon mixing of the two components in *d*₆-benzene at rt (NMR: δ –7.0 (¹¹B), δ –2.4, –16.3 (³¹P), for further details see the Supporting Information). Heating of the sample at 60 °C overnight eventually resulted in the 1,1-carboboration reaction with a practically complete conversion to the new ring enlarged FLP **11a** (see Scheme 3). We prepared compound **11a** on a

Scheme 3



preparative scale from **10a** and **3** in toluene (70 °C, overnight) and isolated the P/B/P FLP **11a** in 75% yield. It was characterized by X-ray diffraction (see Figure 3 and Table 1). The X-ray crystal structure analysis has shown that a 1,1-carboboration reaction has occurred with migration of the CH₂CH₂–Pmes₂ group to an acetylenic carbon atom. The newly formed (“inserted”) substituted exomethylene group (C1=C2) is formed stereoselectively with the Ph₂P substituent and the remaining B(C₆F₅)₂ functionality oriented *cis* to each other. Consequently, compound **11a** features a marked P1–B1 interaction resulting in a central monounsaturated four-

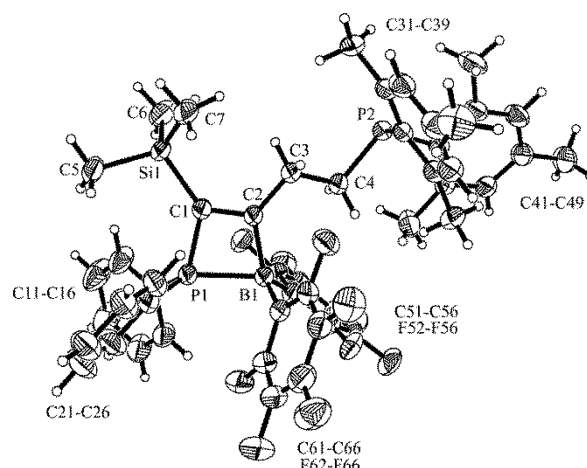


Figure 3. View of the molecular structure of the P/B/P FLP **11a** (thermal ellipsoids are shown with 30% probability).

Table 1. Selected Structural Parameters of the P/B/P FLPs **11a** (PPh₂) and **11b** (P(*o*-tol)₂) and the Intermolecular H₂ Activation Product **13**^a

compd	11a	11b	13
P1–B1	2.028(3)	2.057(4)	2.025(4)
P1–C1	1.790(3)	1.792(3)	1.786(3)
C1–C2	1.367(3)	1.356(5)	1.370(4)
C2–B1	1.647(4)	1.635(5)	1.640(5)
B1–P1–C2	78.9(1)	77.8(2)	79.0(1)
C2–B1–P1	43.4(1)	42.9(1)	43.4(1)
P1–C1–C2–B1	–1.6(2)	3.5(3)	–5.9(3)
C2–C3–C4–P2	–179.0(2)	173.9(2)	–170.7(2)

^aBond lengths in Å; angles and dihedral angles in deg.

membered P/B containing heterocycle.³ The more bulky pendant Pmes₂ group contains a tricoordinate phosphorus center with a typical trigonal-pyramidal coordination geometry ($\Sigma P2^{CCC} = 314.7^\circ$).

The intramolecular Ph₂P/B(C₆F₅)₂ coordination of **11a** is retained in solution. This has become evident from the typical NMR features (³¹P: δ 14.0 (PPh₂) and δ –21.0 (Pmes₂); ¹⁰B: δ –6.3; ¹⁹F: δ –129.6 (*o*), –157.7 (*p*), –163.9 (*m*) of C₆F₅, $\Delta\delta^{19}F(m, p) = 6.2$ ppm). The bridging C=C unit gives rise to ¹³C NMR resonances at δ 209.4 (=C[B]) and δ 136.6 (=C[P]), ¹J_{PC} = 27.3 Hz), respectively, and we have observed the typical ¹H NMR signals of the pendant CH₂CH₂–[P] moiety at δ 3.05 and 2.76.

The markedly more bulky di(*o*-tolyl)phosphino-(trimethylsilyl)acetylene reagent **10b** reacts analogously with the FLP **3** to directly give the extended P/B/P FLP **11b** that was isolated in 81% yield. It shows similar spectroscopic data (see the Supporting Information for details) and structural parameters (see Table 1; the structure of compound **11b** is depicted in the Supporting Information).

The unsaturated vicinal P/B FLPs **1** are not very reactive.^{2,3} They usually only show a small spectrum of the typical FLP reactivity among that being the 1,2-addition of an aldehyde¹⁸ or the above-mentioned cooperative P/B addition to isonitriles.² The new unsaturated P/B/P FLP **11a** is no exception, but as expected, it cleanly reacted with *n*-butylisocyanide to give the five-membered heterocyclic product **12** (see Scheme 3) that we isolated as colorless crystals in 40% yield. The X-ray crystal structure analysis shows that a pair of new bonds (P1–C5 and

B1–C5) have been formed to the carbon atom of the incoming isonitrile reagent (see Figure 4 and Table 2). This has resulted

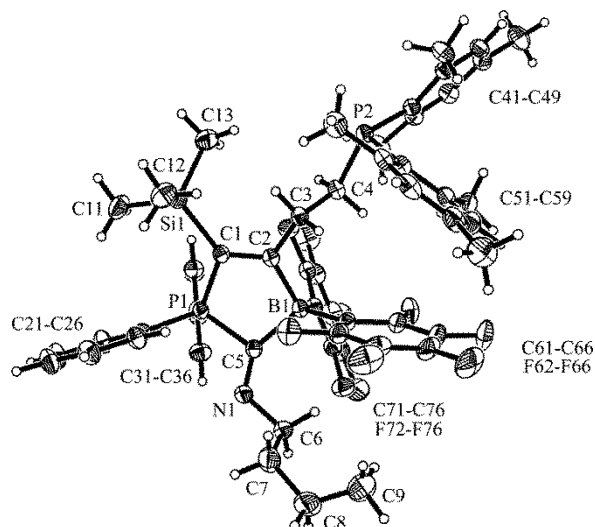


Figure 4. Molecular structure of the isonitrile addition product **12** (thermal ellipsoids are shown with 30% probability).

Table 2. Selected Structural Parameters of the Isonitrile Addition Products **12** and **18** (see Schemes 3 and 5)^a

compd	12	18
C1–P1	1.777(3)	1.776(2)
C1–C2	1.362(4)	1.362(3)
C2–B1	1.649(4)	1.654(3)
B1–C5	1.664(4)	1.651(3)
C5–P1	1.840(3)	1.838(2)
C5–N1	1.266(3)	1.270(3)
C1–P1–C5	97.5(1)	97.3(1)
C2–B1–C5	100.1(2)	100.0(2)
P1–C5–B1	102.7(2)	103.1(1)
B1–C5–N1	142.4(3)	142.7(2)
P1–C5–N1	114.8(2)	114.1(2)
C5–N1–C6	120.8(2)	121.6(2)
P1–C5–N1–C6	−177.4(2)	−175.8(2)
B1–C5–N1–C6	−1.1(6)	−1.0(4)
C2–C3–C4–P2	172.5(2)	−178.1(2) ^b
ΣP2 ^{CCC}	314.4	–

^aBond lengths in Å; angles and dihedral angles in deg. ^bC2–C3–C4–C41.

in the formation of the central five-membered heterocyclic core of compound **12** that contains a total of three sp²-hybridized carbon atoms (C1, C2, C5). The resulting C(5)=N(1) double bond is oriented slightly unsymmetrically at the central core, leaning over toward the phosphorus side. It appears as if the μ-(RC=N) group was experiencing a “memory effect”, having been attacked by the phosphorus nucleophile after being activated by coordination to the boron Lewis acid. We have observed the *E* isomer of the resulting imine-like structure.

In solution we can also only identify one isomer of **12**. It is characterized by a ¹³C NMR (R–C=N) resonance at δ 193.6. The core heteroatom NMR features occur at δ −14.6 (¹¹B) and δ 22.1 (³¹P (1:1:1:1 quartet)). The ³¹P NMR signal of the pendant Pmes₂ group was located at δ −21.1 and compound **12** exhibits a ²⁹Si NMR resonance at δ −9.3.

In contrast to the C₃-bridged P/B FLP **6** (see above), the P/B/P FLP **11a** does not react with dihydrogen under similar conditions. This is probably due to deactivation of the boron Lewis acid by internal interaction with the adjacent relatively small PPh₂ phosphanyl Lewis base. However, addition of one molar equivalent of the strong boron Lewis acid B(C₆F₅)₃ gave an intermolecular FLP.¹⁹ Exposure of the **11a**/B(C₆F₅)₃ mixture to H₂ at ambient conditions gave the respective phosphonium/hydridoborate salt **13** (isolated in 87% yield) (see Scheme 3).

The NMR spectra show the typical [P]–H and [B]–H signals: δ −25.4 (¹¹B, ¹J_{BH} ~ 90 Hz) and δ −12.2 (³¹P, ¹J_{PH} = 476 Hz). The spectra also show that the Ph₂P···B(C₆F₅)₂ unit of the central four-membered core structure has remained largely unaffected by the reaction. Consequently, we have monitored the typical ³¹P (δ 13.1, PPh₂) and ¹¹B (δ −7.4, B(C₆F₅)₂) NMR signals of this unit of compound **13** [cf. starting material **11a**: ³¹P: δ 14.0 (PPh₂) and ¹¹B: δ −6.3 (B(C₆F₅)₂)].

The intact four-membered core structure of compound **13** has been confirmed by X-ray crystal structure analysis (see Figure 5). The core structural features of **13** are very similar to

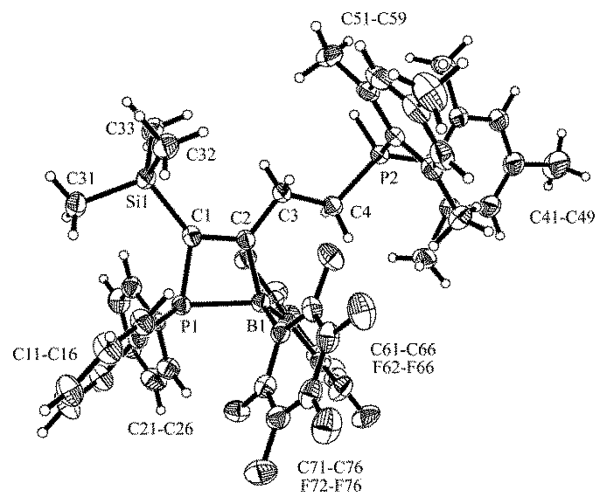
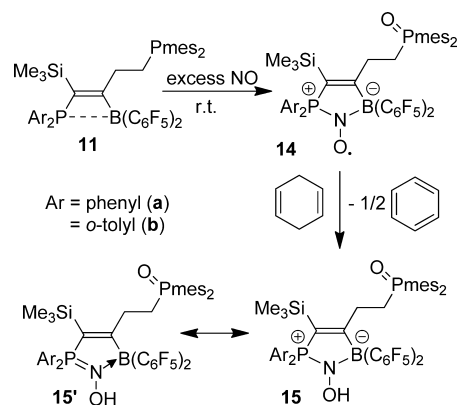


Figure 5. Molecular structure of the cation of the phosphonium/hydridoborate salt **13** (thermal ellipsoids are shown with 30% probability).

those of the parent compounds **11a** (see Table 1). The pendant CH₂CH₂–P⁺Hmes₂ substituent of **13** contains a pseudotetrahedral phosphonium center (ΣP2^{CCC} = 341.3°). The structure contains the [HB(C₆F₅)₃][−] counteranion with a pseudotetrahedral boron center (ΣB2^{CCC} = 333.2°). We note that, in the crystal, there seems to be a rather short distance between the phosphonium proton [P]–H and the borate hydride H–[B] (*d* P2–H···H–B2 = 2.244 Å).

Reactions of the P/B/P-Frustrated Lewis Pairs **11 with Nitrogen Monoxide.** The unsaturated vicinal P/B FLPs **1** so far have not been shown to be able to add to NO. This is surprisingly different with the P/B/P FLPs **11** although they contain the same type of a central P/B FLP core. The compounds **11** react cleanly with nitrogen monoxide. As a typical example, we have exposed a benzene solution of the P/B/P FLP **11a** to an atmosphere of NO (1.5 bar) overnight at rt. Workup with pentane eventually gave the persistent FLPNO aminoxyl radical **14a** as a pale blue-green solid that was isolated in 81% yield (Scheme 4).

Scheme 4



The persistent aminosyl radical **14a** was characterized by X-ray diffraction (see Figure 6 and Table 3). The X-ray crystal

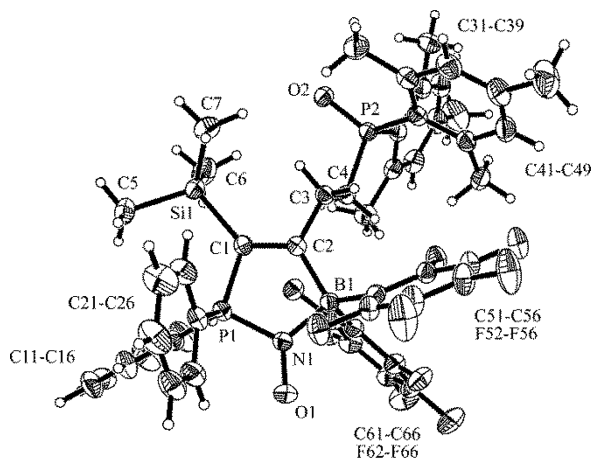


Figure 6. Molecular structure of the persistent P/B/PO FLPNO aminosyl radical **14a** (thermal ellipsoids are shown with 30% probability).

Table 3. Selected Structural Parameters of the P/B/PO FLPNO Aminosyl Radicals **14a** (Ar = PPh₂) and **14b** (Ar = P(*o*-tolyl)₂) and Their Corresponding FLPNOH Products **15a**, **b**^a

compd	14a	15a	14b	15b
N1–O1	1.292(2)	1.431(3)	1.299(5)	1.436(2)
P1–N1	1.694(2)	1.647(2)	1.676(4)	1.642(2)
B1–N1	1.570(2)	1.557(4)	1.571(7)	1.560(3)
C1–P1	1.774(2)	1.789(3)	1.790(5)	1.790(2)
C1–C2	1.368(2)	1.353(4)	1.379(6)	1.362(3)
C2–B1	1.637(2)	1.635(4)	1.630(8)	1.635(3)
P2–O2	1.489(1)	1.491(2)	1.482(3)	1.479(2)
B1–N1–P1	114.3(1)	109.9(2)	110.5(3)	111.0(1)
B1–N1–O1	126.2(1)	121.2(2)	126.8(4)	121.2(2)
P1–N1–O1	119.3(1)	111.2(2)	122.1(3)	114.5(1)
C2–C3–C4–P2	170.7(2)	–165.7(2)	170.1(3)	168.5(2)
ΣP2 ^{CCC}	323.2	320.8	323.8	323.2
ΣN1 ^{POB}	359.9	342.4	359.4	346.7

^aBond lengths in Å; angles and dihedral angles in deg.

structure analysis has shown that the pendant CH₂CH₂–Pmes₂ moiety of the starting material **11a** had been oxidized to the respective CH₂CH₂–P(O)mes₂ phosphine oxide by exposure

to the excess NO. Also, the central B/P Lewis acid/Lewis base pair has undergone a N,N-addition to one equivalent of NO to give the five-membered heterocyclic central core of the FLPNO aminosyl radical **14a**. A close inspection of the characteristic bonding features of **14a** reveals that the NO unit has become rather symmetrically bonded inside this framework. Free NO has a short nitrogen–oxygen bond of 1.15 Å.^{20a} In **14a**, this has become elongated to 1.292(2) Å (4: 1.296(2) Å;^{6b} TEMPO: 1.284(8) Å^{20c}), which is still a reasonably short bond distance, indicating quite substantial π interaction between these atoms.

Compound **14a** was characterized by electron paramagnetic resonance (EPR) spectroscopy (see Figure 7). The X-band

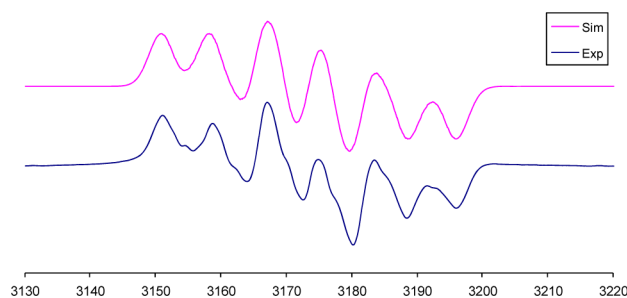


Figure 7. X-band EPR spectrum and simulation for **14a** (fluorobenzene, 10 mM, rt). The sample seems to contain some minor unknown paramagnetic admixture.

EPR spectra of compound **14a** in fluorobenzene at rt shows a signal at $g_{\text{iso}} = 2.0075$ with a distinct hyperfine coupling pattern. Simulation gave $A(^{14}\text{N}) = 20.5$ MHz (4: 18.5 MHz;^{6c} TEMPO: 43.5 MHz^{20b}), $A(^{31}\text{P}) = 47.0$ MHz (4: 48.5 MHz),^{6b} and $A(^{11}\text{B}) = 9.5$ MHz (4: 9.1 MHz).^{6c} This is rather different from some often used organic aminosyl radicals such as TEMPO but close to typical values observed for the FLPNO radical **4** and closely related phosphane/borane FLPNO derivatives.⁶ The Mulliken spin density populations of **14a** were density functional theory (DFT) calculated. Similar to other phosphane/borane FLPNO species,⁶ **14a** is a rather oxygen-centered radical with spin densities at O of 55% and at N of 32% and some rather low contributions at P (ca. 5%) and B (ca. 4%) (for details see the Supporting Information).

The P/B/P system **11b** (Ar = *o*-tolyl) reacts analogously with NO. We have isolated the persistent P/B/PO FLPNO aminosyl radical **14b**, bearing the more bulky P(*o*-tolyl)₂ moiety, as a green solid in 87% yield (see Scheme 4). Compound **14b** was also characterized by X-ray diffraction. Selected structural parameters of **14b** are listed in Table 3. For a view of the molecular structure and further details see the Supporting Information.

The FLPNO radicals **4** (see Scheme 1) behave as typical persistent organic aminosyls (such as e.g. TEMPO or PINO).²¹ They undergo typical radical reactions such as hydrogen atom abstraction from suitable H⁺ donors. The P/B/PO FLPNO radicals **14** behave similarly. In situ generated compound **14a** reacted rapidly with the H atom donor 1,4-cyclohexadiene (30 min, rt) to give the diamagnetic FLPNOH product **15a** that we have isolated as a colorless solid in 69% yield (see Scheme 4). Compound **15a** was characterized by C, H, and N elemental analysis, by spectroscopy, and by X-ray diffraction (see Table 3).

Compound **15a** shows the [N]OH ¹H NMR signal at δ 4.31 (d with a ³J_{PH} = 5.1 Hz coupling constant). It shows ¹⁹F NMR

signals of the pair of symmetry equivalent C_6F_5 groups typical for a tetracoordinated boron geometry (δ -130.8 (*o*), -160.4 (*p*), -164.8 (*m*), $\Delta\delta^{19}F(m, p) = 4.4$ ppm) and a corresponding ^{10}B NMR feature at δ -5.6 . Two ^{31}P NMR signals were located at δ 52.0 ($P(Ph)_2$) and 38.9 ($P(O)mes_2$), and a ^{29}Si NMR resonance was at δ -9.5 .

In the crystal, the structures of the FLPNO radical **14a** and the FLPNOH product **15a** look superficially similar. However, there are a number of significant differences in detail. First, and most importantly, the N1–O1 bond in **15a** is much longer than that in **14a**.⁶ The difference is ~ 0.14 Å, indicating the loss of the electron delocalization between N and O by using the odd electron of **14a** to make the new [N]O–H bond. The P1–N1 bond in **15a** is slightly shorter as compared to **14a** (see Table 3) that may indicate some participation of the phosphinimine resonance structure (**15'**, see Scheme 4). In contrast, compound **14a** seems to be adequately described by the σ -bonded core structure. In **15a**, the B1–N1 bond has largely been unaffected by the change of the bonding situation at the adjacent P–N–OH unit. We also note that, in **15a**, the nitrogen atom N1 exhibits a slightly pyramidalized coordination geometry different from the trigonal-planar situation encountered for nitrogen in **14a** (see Table 3 and Figure 8). The

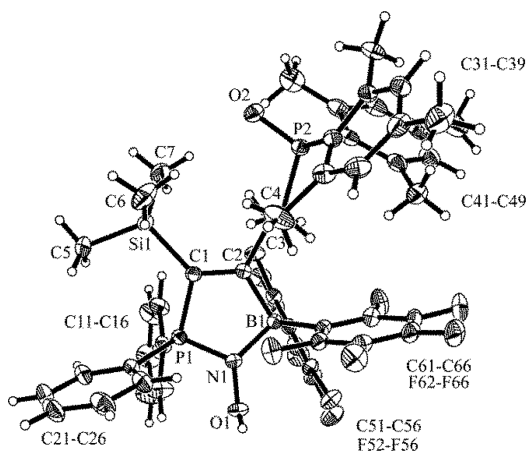


Figure 8. View of the molecular structure of the FLPNOH product **15a** (thermal ellipsoids are shown with 30% probability).

persistent P/B/PO FLPNO aminoxyl radical **14b**, bearing the markedly more bulky $P(o\text{-tolyl})_2$ moiety, reacts analogously with 1,4-cyclohexadiene by H atom abstraction to yield the corresponding diamagnetic FLPNOH product **15b**. Compound **15b** was characterized by NMR spectroscopy (^{10}B : δ -5.3 ; ^{31}P : δ 53.3 ($P(o\text{-tolyl})_2$), 38.6 ($P(O)mes_2$)) and by X-ray diffraction (see Table 3 and the Supporting Information for details).

Solid-State NMR. Figure 9 shows the 1H decoupled ^{11}B and the ^{31}P MAS NMR spectra of compounds **11a**, **15a**, and **25a**. The ^{11}B MAS NMR spectra were influenced by second-order nuclear electric quadrupolar coupling perturbations. The corresponding line shape fit parameters, namely, the quadrupolar coupling constants C_Q , the asymmetry parameters η_Q , and the isotropic chemical shifts δ_{iso} , are summarized in Table 4. The values for **11a** and **25a** are typical for those measured in FLPs with weak intramolecular interactions between vicinal Lewis centers. The ^{11}B C_Q values follow closely the previously established correlations of C_Q and δ_{iso} with the internuclear distance $d(B\cdots P)$ for such systems.² Compound **15a** shows the

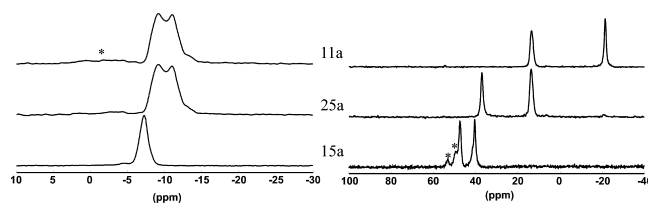


Figure 9. $^{11}B\{^1H\}$ (left) and $^{31}P\{^1H\}$ (right) MAS NMR spectra of compounds **11a** (top), **25a** (middle), and **15a** (bottom). Impurities are indicated by asterisks.

typical spectroscopic behavior of a four-coordinate boron compound.

While neither the ^{11}B nor the ^{31}P NMR spectra give any indication of indirect ^{11}B – ^{31}P spin–spin interactions in **11a**, **15a**, and **25a**, the corresponding coupling constants $^1J(^{31}P$ – $^{11}B)$ can be easily extracted from ^{11}B observed two-dimensional J -resolved spectra (see Figure 10). Values near 50 Hz measured for **11a** and **25a** are typical for similar intramolecular FLPs,²² and for the NO cycloaddition product **15a**, a $^2J(^{11}B$ – $^{31}P)$ value of 27.7 Hz is measured. In addition, J -based $^{31}P/^{11}B$ heteronuclear correlation spectroscopy (HMQC) can be used for the selective detection of those P species interacting covalently with the Lewis acid center, providing an unambiguous assignment of the two ^{31}P signals (see Figures S78–S80 in the Supporting Information). The latter method is particularly useful for compound **15a**, (see Figure S80 in the Supporting Information) where the assignment of the two closely spaced ^{31}P signals is not obvious.

Figure 11 shows the $^{31}P\{^{11}B\}$ REAPDOR (left) and the $^{11}B\{^{31}P\}$ REDOR (right) curves of **11a**, **15a**, and **25a**. The experimental REAPDOR data of **11a** and **25a** show good agreement with simulated curves based on two rather different P \cdots B distances as indicated also by the crystal structure (2.1 and 5.0 Å; dashed and solid curves, respectively). In the case of the $^{31}P\{^{11}B\}$ REAPDOR measurement of **15a**, the data obtained for the remote P atom (40.3 ppm) are best modeled by a ^{31}P (^{11}B)₂ three-spin system based on an intramolecular distance of 5.24 Å, an intermolecular distance of 5.93 Å, and an angle of 119.8° between the two internuclear vectors as deduced from the crystal structure. In contrast, the REAPDOR curve observed for the 47.3 ppm resonance is satisfactorily modeled just by a two-spin system (2.68 Å), which completely dominates the interaction.

The $^{11}B\{^{31}P\}$ REDOR curves (right parts of Figure 11) also agree well with those predicted from the molecular distance geometry (see Table 4). In all three cases, the simulations are based on the full intramolecular $^{11}B^{31}P_2$ three-spin systems. The angles between the dipolar vectors are given as 127.6°, 129.1°, and 105.6° for **11a**, **15a**, and **25a**, respectively. For compound **17**, for which no crystal structure was available, the REDOR data are consistent with a B–P distance of 2.10 Å (see the Supporting Information).

Altogether, all the solid-state NMR results, both on the FLPs **11a** and **25a** as well as on the NO cycloaddition product **15a**, indicate the absence of any covalent interactions between the boron Lewis acid center and the more remote pendant phosphorus Lewis base center in the solid state.

Mechanistic Studies. Since the P/B FLPs **1** that we had previously described were inert toward NO in contrast to our new P/B/P FLPs **11**, it appeared that the pendant CH_2CH_2 – $Pmes_2$ group played a vital role in the formation of the P/B/PO

Table 4. ^{11}B – ^{31}P Distances (Å) from the Crystal Structure (d_{cryst}) and from $^{31}\text{P}\{^{11}\text{B}\}$ REAPDOR (d_{NMR}), Isotropic Indirect Dipolar-Coupling Constants $J(^{11}\text{B}$ – $^{31}\text{P})$ (Solid) and $J(^{31}\text{P}$ – $^{31}\text{P})$ (Solution/Solid) (± 0.5 Hz), Isotropic Chemical Shifts $\delta_{\text{iso}}^{31\text{P}}$ (solution^a; solid^b) and $\delta_{\text{iso}}^{10\text{B}/^{11}\text{B}}$ (Solution/Solid) (± 0.5 ppm), ^{11}B Nuclear Electric Quadrupolar Coupling Constant C_q (± 0.10 MHz), and Electric Field Gradient Asymmetry Parameter η_Q (± 0.10)

	d_{cryst}	d_{NMR}	$J^{11\text{B}^{31}\text{P}}$	$J^{31\text{P}^{31}\text{P}}$	$\delta_{\text{iso}}^{10\text{B}/^{11}\text{B}}$	$\delta_{\text{iso}}^{31\text{P}^a}$	$\delta_{\text{iso}}^{31\text{P}^b}$	C_q	η_Q
11a	2.03	2.10 ^c	48.7	6.3/7.8	–6.3/	14.0	13.4	1.34	0.3
	5.03	5.0 ^d			–7.5	–21.0	–21.4		
25a	2.02	2.10 ^c	49.6	0/0	–6.5/	37.4	37.0	1.31	0.32
	4.96	5.0 ^d			–7.4	13.4	13.5		
15a	2.62	2.70 ^c	27.7	1.9/0	–5.6/	52.0	47.3	0.71	0.82
	5.24	5.2 ^d			–6.2	38.9	40.3		
17	^e	2.10 ^c	50.3	–	–6.2/	14.4	13.1	1.31	0.41
					–7.1				

^aSolution. ^bSolid. ^c ± 0.05 Å. ^d ± 0.1 Å. ^eNo single-crystal structure available.

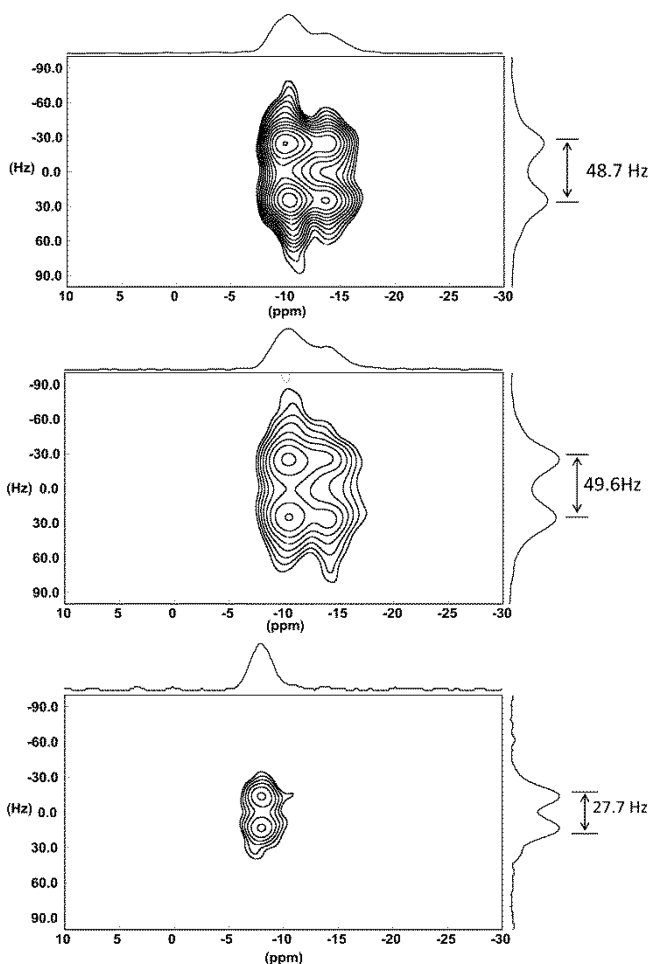


Figure 10. $^{11}\text{B}/^{31}\text{P}$ heteronuclear J -resolved spectra of compounds 11a (top), 25a (middle), and 15a (bottom). The J -coupling doublets extracted from these data are shown in the figure.

FLPNO product. This became supported by a series of additional reactions. We first prepared the unsaturated vicinal P/B FLP 17. This compound is in many details similar to the P/B/P FLP 11, only that it contains a nonfunctionalized pendant CH_2CH_2 –Ph substituent instead of the CH_2CH_2 –Pmes₂ functional group.

Compound 17 was prepared by 1,1-carbo-boration of the borane 16 (i.e., the $\text{HB}(\text{C}_6\text{F}_5)_2$ hydroboration product of styrene)^{23,24} with diphenylphosphino(trimethylsilyl)acetylene (10a) (70 °C, 26 h). It was isolated in 82% yield (^{31}P NMR: δ

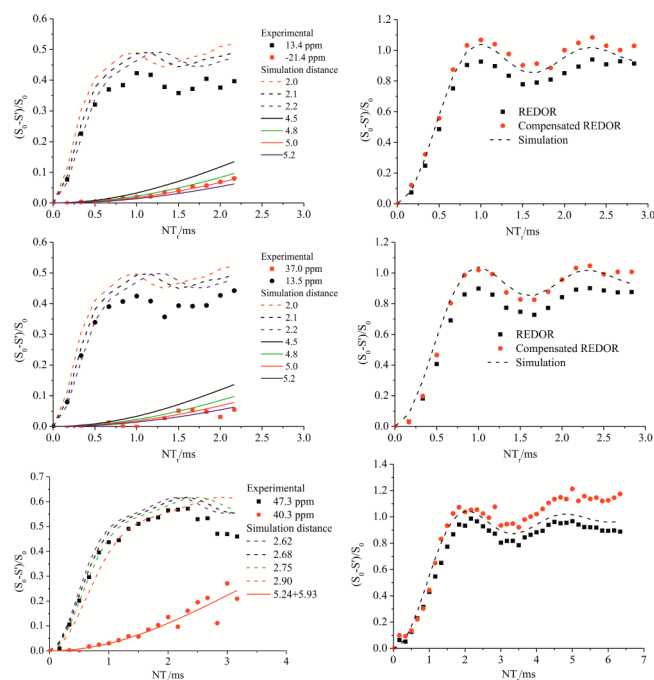
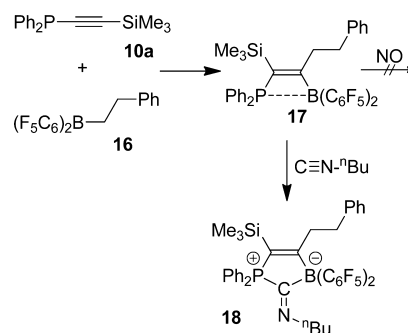


Figure 11. $^{31}\text{P}\{^{11}\text{B}\}$ REAPDOR (left) and $^{11}\text{B}\{^{31}\text{P}\}$ REDOR (right) experimental data points and simulated curves, for compounds 11a (first row), 25a (middle row), and 15a (bottom row). See text for further details.

14.4; ^{10}B : δ –6.2; for further characterization see the Supporting Information). Since we did not get single crystals suitable for characterizing 17 by X-ray diffraction, we prepared its *n*-butylisocyanide addition product 18 (see Scheme 5) (^{13}C

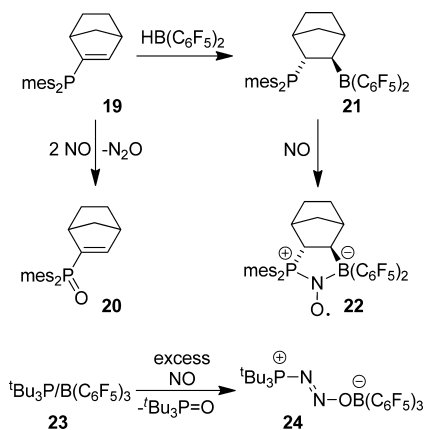
Scheme 5



NMR: δ 194.2 (C=N); ^{10}B : δ -14.4 ($^2J_{31\text{P}10\text{B}} \sim 16$ Hz); ^{31}P : δ 22.7 (1:1:1:1 q, $^2J_{31\text{P}11\text{B}} \sim 51$ Hz)). Compound **18** was characterized by X-ray diffraction (see Table 2 and the Supporting Information for details). This derivatization reaction further confirmed the formation of the P/B FLP **17** by 1,1-carbaboration (see Scheme 5). It turned out that the P/B FLP **17** was indeed inert toward nitrogen monoxide under our typical reaction conditions.

Free phosphanes react readily with NO to form phosphine oxides and N_2O . The mechanistic course of this phosphane oxidation reaction had been carefully examined.¹⁷ We had recently shown that the alkenyl phosphane **19** (see Scheme 6) reacts with NO to give the phosphine oxide **20** (and probably N_2O).^{6f}

Scheme 6



It was shown that this was kinetically a third-order reaction, first order in the phosphane and second order in nitric oxide. Treatment of the phosphane **19** with Piers' borane [$\text{HB}(\text{C}_6\text{F}_5)_2$] gave the saturated vicinal FLP **21**, which reacted with NO following a second-order rate law (first order in the FLP and first order in NO) to give the persistent FLPNO radical **22**.^{6f} We were able to detect the coproduct N_2O in the reaction of the intermolecular FLP $^t\text{Bu}_3\text{P}/\text{B}(\text{C}_6\text{F}_5)_3$ (**23**) with excess NO to give the phosphine oxide $^t\text{Bu}_3\text{P}=\text{O}$ and the known^{6b} FLP- N_2O trapping product **24**.^{6c}

Therefore, it was tempting to assume that oxidation of the free pendant $\text{CH}_2\text{CH}_2\text{-Pmes}_2$ phosphane to the $\text{CH}_2\text{CH}_2\text{-P}(\text{O})\text{mes}_2$ phosphine oxide might be the initial step in the overall reaction of the P/B/P FLPs **11** with nitric oxide. We were able to confirm that experimentally. We exposed the FLP **11a** to 2.2 molar equiv of NO gas at -78 °C. The mixture was slowly warmed to rt and stirred for some time to give a practically quantitative conversion to the P/B/PO FLP product **25a** (see Scheme 7). From the reaction mixture, we isolated compound **25a** in 82% yield. Single crystals of **25a** were obtained from dichloromethane/pentane by the diffusion method.

In the crystal, compound **25a** shows an intact central four-membered heterocyclic FLP structure (similar to the starting material **11a**), with a marked P \cdots B interaction. A pendant $-\text{CH}_2\text{CH}_2-$ unit is attached at the unsaturated C1=C2 unit of the FLP core that has the $\text{P}(\text{O})\text{mes}_2$ phosphine oxide functional group at its end (see Figure 12 and Table 5).

In solution, the NMR features of the four-membered core structure of compound **25a** are quite similar to those of its precursor **11a**. Compound **25a** shows a ^{31}P NMR signal at δ

Scheme 7

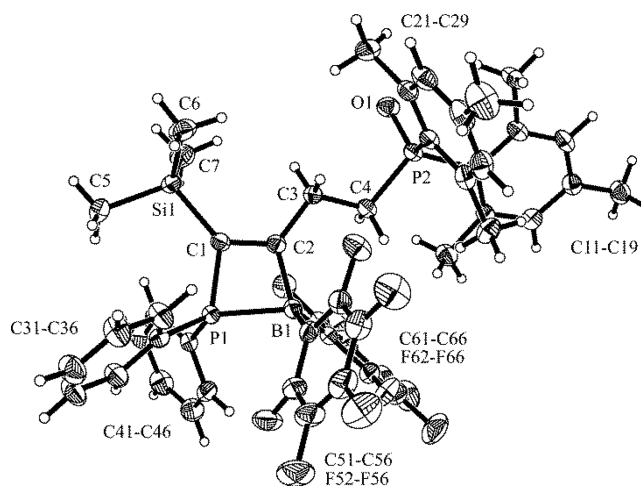
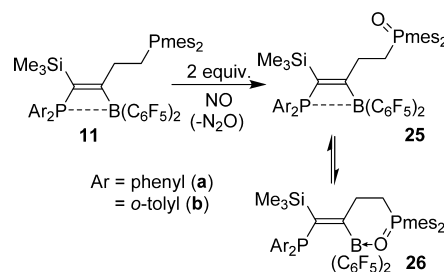


Figure 12. Molecular structure of the P/B/PO FLP **25a** (thermal ellipsoids are shown with 30% probability).

Table 5. Selected Structural Data of the P/B/PO FLPs **25a** (Ar = PPh₂) and **25b** (Ar = P(o-tolyl)₂) and the Related P/B/PS FLP **28a** (Ar = PPh₂)^a

compd	25a	25b	28a
P1-B1	2.024(4)	2.061(3)	2.023(3)
C1-P1	1.793(4)	1.796(2)	1.788(3)
C2-B1	1.643(6)	1.629(4)	1.651(4)
C1-C2	1.368(5)	1.358(3)	1.368(4)
P2-O2	1.481(3)	1.484(2)	1.955(1) ^b
C4-P2	1.816(4)	1.822(2)	1.835(3)
C1-P1-B1	78.9(2)	77.3(1)	79.1(1)
P1-B1-C2	78.8(2)	78.5(1)	78.7(2)
$\Sigma\text{P}2^{\text{CCC}}$	322.1	319.9	318.2
B1-C2-C1-P1	-3.7(3)	-7.9(2)	-1.4(2)
C2-C1-P1-B1	3.0(2)	6.1(2)	1.1(2)
C2-C3-C4-P2	-173.0(3)	171.5(2)	-175.8(2)

^aAngles and dihedral angles in deg; bond lengths in Å. ^bP=S.

13.4 of the central PPh₂-B(C₆F₅)₂ unit with a ^{10}B NMR signal at δ -6.5 (**11a**: δ 14.0 (PPh₂), δ -6.3 B(C₆F₅)₂). The terminal $\text{P}(\text{O})\text{mes}_2$ group gives rise to a ^{31}P NMR signal at δ 37.4. However, compound **25a** shows temperature-dependent ^{31}P NMR spectra (see Figure 13). Below -10 °C, we see a 1:1 intensity pair of new ^{31}P NMR signals appear along with the PPh₂/P(O)mes₂ pair of **25a** that rapidly increase with decreasing temperature. At -80 °C, the new equilibrium component (**26a**) is the major product (**25a/26a** \sim 1:3.5 at -80 °C). From a van't Hoff plot, we have determined the thermodynamic parameters $\Delta H = -4.5$ kcal mol⁻¹ and $\Delta S^0 = -21.0$ cal K⁻¹ mol⁻¹ for the **25a** \rightleftharpoons **26a** equilibrium.

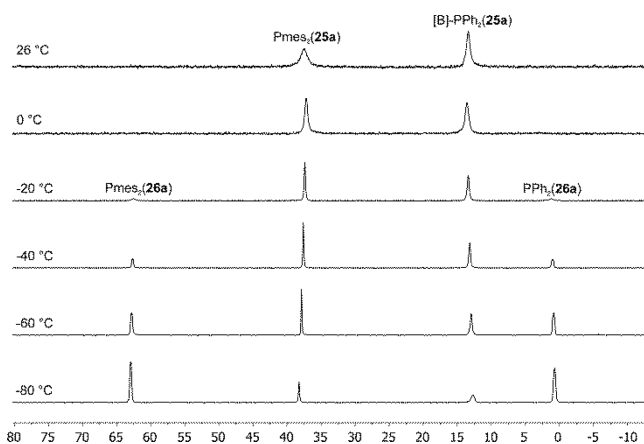


Figure 13. Temperature-dependent ^{31}P NMR spectra of the $25\text{a} \rightleftharpoons 26\text{a}$ equilibrium (in d_8 -toluene).

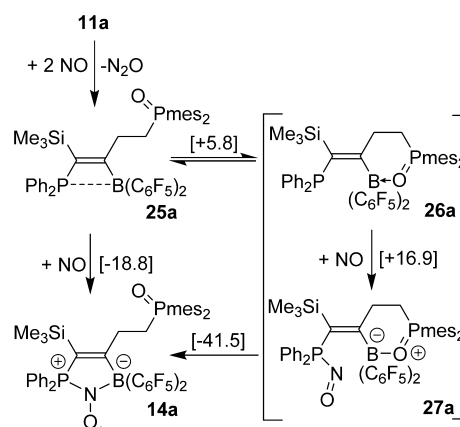
We assume that compound **26a** is the B–O–P bonded isomer of **25a**.²⁵ This is supported by the characteristic ^{31}P NMR signal of the P(O)mes₂ resonance of **26a** at 62.9 that is similar to the corresponding B–O–Pmes₂ signal of the model compound **9** (^{31}P : δ 62.4 (P(O)mes₂); see Scheme 2). The $25\text{a} \rightleftharpoons 26\text{a}$ situation was modeled by DFT calculation. This revealed that the formation of the B–O isomer **26a** is only slightly endothermic in solution (benzene) at ambient temperature ($\Delta\Delta G$ ($25\text{a}/26\text{a}$) calcd. (298 K) = 5.8 kcal mol⁻¹, for further details of the DFT analysis see ref 26 and the Supporting Information).

The P(*o*-tolyl)₂-containing P/B/P FLP **11b** reacted analogously with NO (2.2 molar equiv) under our carefully controlled reaction conditions. The product **25b** (see Scheme 7) was isolated in 85% yield as a colorless solid. It was also characterized by X-ray diffraction (for details see Table 5 and the Supporting Information). In solution, compound **25b** also equilibrates with its isomer **26b**. However, in this case, the $25\text{b} \rightleftharpoons 26\text{b}$ equilibrium lies markedly on the **25b** side. At $-80\text{ }^\circ\text{C}$, we have monitored compound **25b** as the major component by ^{31}P NMR spectroscopy (δ 18.3 (P(*o*-tolyl)₂), δ 37.8 (P(O)mes₂) and the minor compound **26a** (δ -12.2 (P(*o*-tolyl)₂), δ $+62.4$ (P(O)mes₂)) in a $25\text{b}/26\text{b}$ ratio of approximately 7:1. These results show that Pmes₂ oxidation by the typical reaction of a free phosphane with two molar equivalents of NO (probably with formation of N₂O) is initiating the overall reaction sequence of the formation of the P/B/PO FLPNO radicals **14** from the P/B/P FLPs **11**. The presence of the pendant phosphine oxide donor seems essential for activating the FLP Ar₂P···B(C₆F₅)₂ unit. We see this in our experiment of the formation of **26** from **25** (see Schemes 7 and 8).

The possible subsequent reaction course has been studied by DFT calculation (see Scheme 8 and the Supporting Information).²⁶ The B–O–Pmes₂ coordination generates a free PPh₂ functionality available for the phosphane reaction with NO. Formation of the respective Ph₂P–N=O product **27a** is energetically slightly “uphill”, but the subsequent trapping of the coordinated NO by the adjacent borane is strongly exergonic (see Scheme 8). This final step in the formation may take place by a S_Ni-type mechanism, as it is schematically depicted in Scheme 7, or stepwise with reversible opening of the phosphine oxide borane coordination.

Eventually, we have also prepared the respective phosphane sulfide product **28a** by treatment of the P/B/P FLP **11a** with

Scheme 8. Gibbs Free Energies (ΔG , kcal mol⁻¹) at 298 K, in Benzene, DFT Calculated



elemental sulfur. We isolated the P(S)mes₂-substituted FLP **28a** as a colorless solid in 73% yield. It was shown by X-ray diffraction to contain the usual four-membered core structure with a rather long P1–B1 linkage (see Scheme 9, Table 5, and

Scheme 9

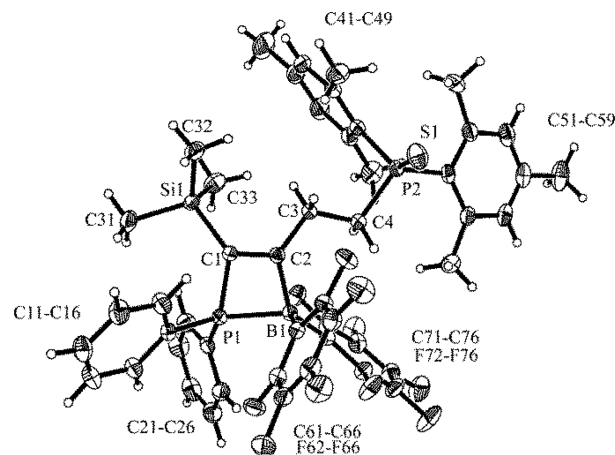
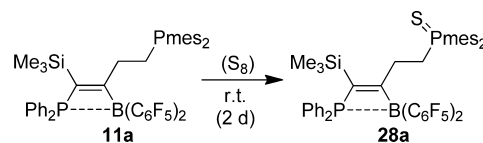


Figure 14. View of the molecular structure of compound **28a** (thermal ellipsoids are shown with 30% probability).

Figure 14). In solution, compound **28a** shows heteronuclear magnetic resonance signals at δ -7.0 (^{10}B), δ 42.8 (^{31}P : P(S)mes₂), δ 13.6 (^{31}P : PPh₂), and δ -10.8 (^{29}Si). The corresponding P(O)mes₂ FLPs **25a, b** \rightleftharpoons **26a, b** react readily with NO to form the corresponding FLPNO radical systems **14a, b**. In contrast, the P(S)mes₂-substituted analogue **28a** did not react with nitrogen monoxide under our typical reaction conditions.

CONCLUSIONS

Our study has shown that the 1,1-carboboration reaction has probably become a versatile tool for modification of FLPs. We have seen that the reaction of the simple parent C₂-bridged FLP mes₂P-CH₂CH₂-B(C₆F₅)₂ (**3**) with the trimethylsilyl-substituted alkyne **5** gave the ring enlarged C₃-bridged new FLP **6**. Formally, the substituted exomethylene containing system **6** contains the vinylidene isomer of the acetylene inserted into the B-C bond;¹⁴ however, this reaction is likely to be mechanistically different, featuring an established pathway of the 1,1-carboboration reaction.^{7,8} The easy synthetic availability of systems like **6** might eventually become significant, since some alkenylborane derivatives were recently shown to be susceptible to nucleophilic attack at an activated carbon position to give borata-alkenes,²⁷ which might eventually add new aspects to FLP chemistry in suitably designed examples.

We have shown that the 1,1-carboboration reaction of **3** with phosphanyl-substituted silylacetylenes readily takes place. The CH₂CH₂-Pmes₂ group becomes transferred to carbon in this reaction, and we have achieved an easy entry to P/B/P FLPs **11**. In contrast to the simpler C₃-bridged P/B FLPs **6** that proved to be active, for example, in H₂ cleavage, the P/B/P FLPs are much less reactive. However, they undergo a remarkable reaction sequence with nitrogen monoxide, using the pendant CH₂CH₂-Pmes₂ functionality for generating an activation principle for the adjacent dormant P/B FLP in situ. This weakening of the deactivating P...B interaction by a pendant activator group is quite a unique feature. This indicated to us that remote activation of FLP systems might become a useful tool in FLP chemistry.

EXPERIMENTAL SECTION

1,1-Carboration Reactions: Preparation of Compounds 6, 11a, b, and 17. *In Situ Generation of Compound 3.* HB(C₆F₅)₂ (1 equiv) and dimesityl(vinyl)phosphane (1 equiv) were both dissolved in the respective solvent, and then the solutions were combined at rt and stirred for ~15 min at this temperature. Subsequently, the solution was used for further reactions.

Synthesis of Compound 6. Compound **3** was generated in situ as described above (HB(C₆F₅)₂: 34.6 mg, 0.1 mmol; dimesityl(vinyl)phosphane: 29.6 mg, 0.1 mmol; solvent: C₆D₆) and combined with trimethyl(phenylethynyl)silane (**5**, 17.3 mg, 0.1 mmol, 1 equiv) at room temperature. The resulting solution was heated to 60 °C overnight and then investigated by NMR spectroscopic experiments. Then, all volatiles were removed in vacuo, and the residue dried in vacuo that gave compound **6** as a yellow solid (60.0 mg, 0.07 mmol, 73%). Anal. Calcd for C₄₃H₄₀BF₁₀P₂Si: C, 63.24; H, 4.94. Found: C, 63.27; H, 5.34. ¹H NMR (500 MHz, C₆D₆, 299 K): δ = 7.22 (2H), 7.06 (1H), 6.90 (2H) (Ph), 6.40 (d, ⁴J_{PH} = 3.1 Hz, 4H, *m*-mes), 2.61 (m, 2H, =CH₂), 2.43 (m, 2H, PCH₂), 1.90 (s, 6H, *p*-CH₃^{mes}), 1.89 (s, 12H, *o*-CH₃^{mes}), -0.14 (s, ²J_{SiH} = 6.4 Hz, SiCH₃). ¹³C{¹H} NMR (126 MHz): δ = 161.4 (br, =CB), 149.1 (d, ⁵J_{PC} = 0.9 Hz, *i*-Ph), 148.3 (d, ⁴J_{PC} = 14.9 Hz, =CSi), 142.1 (d, ¹J_{PC} = 8.4 Hz, *o*-mes), 140.3 (d, ⁴J_{PC} = 2.3 Hz, *p*-mes), 130.8 (d, ³J_{PC} = 8.0 Hz, *m*-mes), 128.7 (d, ¹J_{PC} = 34.2 Hz, *i*-mes)¹, 128.6, 127.7, 125.3 (Ph), 36.4 (d, ²J_{PC} = 11.9 Hz, =CH₂), 26.9 (d, ¹J_{PC} = 26.1 Hz, PCH₂), 23.8 (d, ³J_{PC} = 5.7 Hz, *o*-CH₃^{mes}), 20.4 (d, ²J_{PC} = 1.0 Hz, *p*-CH₃^{mes}), 1.1 (SiCH₃). ¹⁹F NMR (470 MHz): δ = -123.3 (*o*), -156.9 (*p*), -164.1 (*m*), [Δδ¹⁹F_{m,p} = 7.2]. ¹¹B{¹H} NMR (160 MHz): δ = 4.7. ³¹P{¹H} NMR (202 MHz): δ = 26.5. ²⁹Si{DEPT} NMR (99 MHz): δ = -9.5.

Synthesis of Compound 11a, b. General Procedure. Compound **3** was generated in situ as described above (HB(C₆F₅)₂: 34.6 mg, 0.1 mmol; dimesityl(vinyl)phosphane: 29.6 mg, 0.1 mmol; solvent: toluene). Then, a solution of the respective diaryl((trimethylsilyl)ethynyl)phosphane (**10a**: 282 mg, 1.0 mmol, 1 equiv; **10b**: 310 mg, 1.0 mmol, 1 equiv) in toluene (ca. 2 mL) was added, and the resulting

slightly yellow solution was stirred at 70 °C for overnight. ³¹P NMR experiments indicated complete conversion on the next day. After all volatiles were removed in vacuo, the obtained residue was suspended in *n*-pentane (ca. 5 mL) and sonicated for 10 min. Then, the supernatant was taken off, and the remaining solid was washed with *n*-pentane (2 × 5 mL).

Compound 11a. Drying of the remaining solid in vacuo gave **11a** (690 mg, 0.75 mmol, 75%) as a colorless solid. mp: 121 °C. Anal. Calcd for C₄₉H₄₅BF₁₀P₂Si: C, 63.64; H, 4.91. Found: C, 64.09; H, 5.07. ¹H NMR (500 MHz, C₆D₆, 299 K): δ = 7.25 (4H), 6.90 (2H), 6.83 (4H) (Ph), 6.65 (dm, ⁴J_{PH} = 2.7 Hz, 4H, *m*-mes), 3.05 (m, 2H, =CH₂), 2.76 (m, 2H, PCH₂), 2.32 (s, 12H, *o*-CH₃^{mes}), 2.06 (s, 6H, *p*-CH₃^{mes}), 0.02 (s, ²J_{SiH} = 6.6 Hz, 9H, SiCH₃). ¹³C{¹H} NMR (126 MHz): δ = 209.4 (br, =CB), 142.0 (d, ²J_{PC} = 13.5 Hz, *o*-mes) 137.7 (*p*-mes), 136.6 (d, ¹J_{PC} = 27.3 Hz, =CSi), 133.1 (d, ¹J_{PC} = 23.0 Hz, *i*-mes), 132.0 (d, ²J_{PC} = 9.1 Hz, *o*-Ph), 131.5 (d, ⁴J_{PC} = 2.8 Hz, *p*-Ph), 130.5 (d, ⁴J_{PC} = 2.8 Hz, *m*-mes), 128.8 (d, ³J_{PC} = 10.2 Hz, *m*-Ph), 127.4 (d, ¹J_{PC} = 37.9 Hz, *i*-Ph), 37.9 (dd, ³J_{PC} = 52.1 Hz, ²J_{PC} = 23.1 Hz, =CH₂), 27.4 (d, ¹J_{PC} = 17.0 Hz, PCH₂), 23.0 (d, ³J_{PC} = 13.6 Hz, *o*-CH₃), 20.8 (*p*-CH₃), -0.1 (d, ³J_{PC} = 2.0 Hz, ¹J_{SIC} = 52.6 Hz, SiCH₃). ¹⁹F NMR (470 MHz): δ = -129.6 (*o*), -157.7 (*p*), -163.9 (*m*), [Δδ¹⁹F_{m,p} = 6.2]. ¹⁰B{¹H} NMR (54 MHz): δ = -6.3. ³¹P{¹H} NMR (202 MHz): δ = 14.0 (PPh₂), -21.0 (d, ⁵J_{PP} = 6.3 Hz, Pmes₂). ²⁹Si{¹H} DEPT (99 MHz): δ = -11.4 (d, ²J_{PSi} = 6.5 Hz).

Compound 11b. The combined washing solutions were kept at -40 °C for overnight, and the obtained precipitate was collected. Both the dried precipitate and the previously isolated solid gave compound **11b** (773 mg, 0.8 mmol, 81%) as a colorless solid. mp: 81 °C. Anal. Calcd for C₅₁H₄₉BF₁₀P₂Si: C, 64.29; H, 5.18. Found: C, 64.26; H, 5.18. ¹H NMR (600 MHz, tol-*d*₈, 299 K): δ = 7.14 (2H), 6.84 (2H), 6.69 (2H), 6.68 (2H) (*o*-tol), 6.61 (d, ⁴J_{PH} = 2.6 Hz, 4H, *m*-mes), 2.91 (br, 2H, =CH₂), 2.78 (br, 2H, PCH₂), 2.29 (s, 12H, *o*-CH₃^{mes}), 2.20 (br, 6H, *o*-CH₃^{o-tol}), 2.01 (s, 6H, *p*-CH₃^{mes}), -0.11 (s, ²J_{SiH} = 6.6 Hz, 9H, SiCH₃). ¹³C{¹H} NMR (151 MHz): δ = 206.2 (br, =CB), 142.2 (d, ²J_{PC} = 11.9 Hz, *o*-tol), 141.9 (d, ²J_{PC} = 13.4 Hz, *o*-mes), 137.7 (*p*-mes), 137.2 (d, ¹J_{PC} = 29.0 Hz, =CSi), 133.9 (br d, ²J_{PC} = 5.6 Hz, *o*'-tol), 133.3 (d, ¹J_{PC} = 23.1 Hz, *i*-mes), 131.6 (br d, ³J_{PC} = 8.0 Hz, *m*'-tol), 131.5 (br d, ⁴J_{PC} = 2.6 Hz, *p*'-tol), 130.6 (d, ³J_{PC} = 2.6 Hz, *m*-mes), 126.5 (d, ¹J_{PC} = 35.7 Hz, *i*'-tol), 126.1 (d, ³J_{PC} = 8.4 Hz, *m*'-tol), 118.3 (br, *i*-C₆F₅), 38.0 (dd, ³J_{PC} = 50.5 Hz, ²J_{PC} = 23.3 Hz, =CH₂), 27.0 (d, ¹J_{PC} = 18.7 Hz, PCH₂), 23.3 (d, ³J_{PC} = 13.4 Hz, *o*-CH₃^{mes}), 22.2 (br d, ³J_{PC} = 5.2 Hz, *o*-CH₃^{o-tol}), 20.8 (*p*-CH₃^{mes}), -0.1 (d, ³J_{PC} = 1.8 Hz, ¹J_{SIC} = 53.1 Hz, SiCH₃). ¹⁹F NMR (564 MHz): δ = -128.7 (*o*), -157.5 (*p*), -163.6 (*m*), [Δδ¹⁹F_{m,p} = 6.1]. ³¹P{¹H} NMR (243 MHz): δ = 18.5 (P(*o*-tol)), -19.5 (d, ⁵J_{PP} = 6.8 Hz, Pmes). ¹⁰B{¹H} NMR (64 MHz): δ = -2.3. ²⁹Si{¹H} DEPT (119 MHz): δ = -11.4 (d, ²J_{PSi} = 6.1 Hz).

X-ray Crystal Structure Analysis of Compounds 11a, b. Compound **3** was generated in situ as described above (HB(C₆F₅)₂: 69.2 mg, 0.2 mmol; dimesityl(vinyl)phosphane: 59.3 mg, 0.2 mmol; solvent: *n*-pentane). Then, a solution of the respective diaryl((trimethylsilyl)ethynyl)phosphane (**10a**: 56.5 mg, 0.2 mmol, 1 equiv; **10b**: 62.0 mg, 0.2 mmol, 1 equiv) in *n*-pentane (~2 mL) was added, and the resulting slightly yellow solution was stirred in an autoclave at 70 °C for overnight. After the solution was cooled to rt, it was stored at -40 °C for 2 h, resulting in a colorless precipitate. The supernatant was taken off and stored at -40 °C for 2 days, giving 120 mg (0.13 mmol, 65%) of crystalline material, which was identified as pure **11a** by NMR experiments (**11b**: 105 mg, 0.14 mmol, 71%). The obtained crystals were suitable for the X-ray crystal structure analysis.

Synthesis of Compound 17. Compound **10a** (113 mg, 0.4 mmol, 1 equiv) and PhCH₂CH₂B(C₆F₅)₂ (**16**, 180 mg, 0.4 mmol, 1 equiv) were dissolved separately in toluene (each ca. 2 mL). The solutions were combined at rt and then heated to 70 °C for 2 days. After the solution was cooled to rt, all volatiles were removed in vacuo to give compound **17** (240 mg, 0.33 mmol, 82%) as a yellow solid. Anal. Calcd for C₃₇H₂₈BF₁₀P₂Si: C, 60.67; H, 3.85. Found: C, 60.26; H, 3.96. NMR characterization of compound **17**: An analogous reaction (0.1 mmol reaction size) was carried out in C₆D₆. After heating the sample

for 2 days at 70 °C and subsequent cooling to rt, the solution was characterized by NMR experiments, which showed complete conversion of the starting materials to compound 17. ^1H NMR (500 MHz, C_6D_6 , 299 K): δ = 7.34 (4H), 6.94 (2H), 6.88 (4H) (Ph^{P}), 7.26 (2H), 7.16 (2H), 7.06 (1H) (Ph), 3.37 (m, 2H, $=\text{CH}_2$), 2.88 (m, 2H, $^{\text{Ph}}\text{CH}_2$), 0.02 (s, $^2J_{\text{SiH}} = 6.7$ Hz, SiCH_3). $^{13}\text{C}\{^1\text{H}\}$ NMR (126 MHz): δ = 208.6 (br, $=\text{CB}$), 141.8 (*i*-Ph), 137.9 (d, $^1J_{\text{PC}} = 27.7$ Hz, $=\text{CSi}$), 132.1 (d, $^2J_{\text{PC}} = 9.1$ Hz, *o*- Ph^{P}), 131.5 (d, $^4J_{\text{PC}} = 3.0$ Hz, *p*- Ph^{P}), 129.0 (*m*-Ph), 128.8 (d, $^3J_{\text{PC}} = 10.2$ Hz, *m*- Ph^{P}), 128.4 (*o*-Ph), 126.9 (d, $^1J_{\text{PC}} = 38.9$ Hz, *i*- Ph^{P}), 126.5 (*p*-Ph), 43.0 (d, $^3J_{\text{PC}} = 49.3$ Hz, $=\text{CH}_2$), 36.1 (d, $^4J_{\text{PC}} = 1.9$ Hz, $^{\text{Ph}}\text{CH}_2$), 0.2 (d, $J = 2.3$ Hz, $^1J_{\text{SiC}} = 53.0$ Hz, SiCH_3). ^{19}F NMR (470 MHz): δ = -129.6 (*o*), -157.3 (*p*), -163.8 (*m*), $[\Delta\delta^{19}\text{F}_{\text{m,p}} = 6.5]$. $^{10}\text{B}\{^1\text{H}\}$ NMR (54 MHz): δ = -6.2. $^{31}\text{P}\{^1\text{H}\}$ NMR (202 MHz): δ = 14.4. $^{29}\text{Si}\{^1\text{H}\}$ DEPT (99 MHz): δ = -11.3 (d, $^2J_{\text{PSi}} = 6.5$ Hz).

Reactions of Compounds 11a and 17 with Isocyanide.

Caution! Many isocyanides are toxic compounds that need to be handled with due care.

Synthesis of Compound 12. Compound 3 and compound 11a were generated in situ as described above ($\text{HB}(\text{C}_6\text{F}_5)_2$: 69.2 mg, 0.2 mmol; dimesityl(vinyl)phosphane: 59.3 mg, 0.2 mmol; compound 10a: 56.2 mg, 0.2 mmol; solvent: toluene). Then, *n*-butylisocyanide (21.0 μL , 0.2 mmol, 1 equiv) was added, and the solution was stirred for 1 h at rt. Subsequently, all volatiles were removed in vacuo. The obtained solid was taken up in *n*-pentane (~2 mL) and stored at -40 °C for 2 days. The white precipitate was collected and taken up in *n*-pentane (~2 mL). Slow evaporation of the solvent at -40 °C gave compound 12 (80 mg, 0.08 mmol, 40%) as colorless crystals. Crystals obtained in this way were suitable for the X-ray crystal structure analysis. Anal. Calcd for $\text{C}_{54}\text{H}_{54}\text{BF}_{10}\text{NP}_2\text{Si}$: C, 64.35; H, 5.40; N, 1.39. Found: C, 63.87; H, 5.34; N, 1.23. ^1H NMR (600 MHz, CD_2Cl_2 , 299 K): δ = 7.60 (2H), 7.49 (4H), 7.48 (4H) (Ph), 6.71 (d, $^4J_{\text{PH}} = 2.4$ Hz, 4H, *m*-mes), 3.28 (m, 2H, 1-H), 2.60 (m, 2H, PCH_2), 2.48 (m, 2H, $=\text{CH}_2$), 2.20 (s, 6H, *p*- CH_3^{mes}), 2.11 (s, 12H, *o*- CH_3^{mes}), 1.35 (m, 2H, 2-H), 1.11 (m, 2H, 3-H), 0.74 (t, $^3J_{\text{HH}} = 7.5$ Hz, 3H, 4-H), 0.03 (s, $^2J_{\text{SiH}} = 6.6$ Hz, SiCH_3). $^{13}\text{C}\{^1\text{H}\}$ NMR (151 MHz): δ = 219.1 (br, $=\text{CB}$), 193.6 (br t (1:1:1), $J \sim 45$ Hz, $\text{C}=\text{N}$), 142.0 (d, $^2J_{\text{PC}} = 13.3$ Hz, *o*-mes), 138.0 (*p*-mes), 133.4 (d, $^2J_{\text{PC}} = 9.0$ Hz, *o*-Ph), 133.3 (d, $^4J_{\text{PC}} = 3.1$ Hz, *p*-Ph), 132.7 (d, $^1J_{\text{PC}} = 22.4$ Hz, *i*-mes), 130.1 (d, $^3J_{\text{PC}} = 3.0$ Hz, *m*-mes), 129.3 (d, $^3J_{\text{PC}} = 11.7$ Hz, *m*-Ph), 124.0 (d, $^1J_{\text{PC}} = 73.8$ Hz, *i*-Ph), 58.6 (d, $^3J_{\text{PC}} = 37.2$ Hz, C1), 39.4 (dd, $J_{\text{PC}} = 24.6$ Hz, $J_{\text{PC}} = 23.0$ Hz, $=\text{CH}_2$), 32.8 (d, $^4J_{\text{PC}} = 2.0$ Hz, C2), 26.3 (d, $^1J_{\text{PC}} = 15.5$ Hz, PCH_2), 22.9 (d, $^3J_{\text{PC}} = 13.3$ Hz, *o*- CH_3^{mes}), 20.9 (C3), 20.8 (*p*- CH_3^{mes}), 14.0 (C4), 1.0 (d, $^3J_{\text{PC}} = 2.0$ Hz, $^1J_{\text{SiC}} = 53.1$ Hz, SiCH_3). ^{19}F NMR (564 MHz): δ = -129.0 (*o*), -160.3 (*p*), -165.3 (*m*), $[\Delta\delta^{19}\text{F}_{\text{m,p}} = 5.0]$. $^{11}\text{B}\{^1\text{H}\}$ NMR (192 MHz): δ = -14.6 (d, $^2J_{3\text{IP11B}} = 49.4$ Hz). $^{31}\text{P}\{^1\text{H}\}$ NMR (243 MHz): δ = 22.1 (q 1:1:1:1, $J_{3\text{IP11B}} = 49.4$ Hz, PPh_2), -21.1 (d, $^5J_{\text{PP}} = 4.7$ Hz, Pmes_2). $^{29}\text{Si}\{^1\text{H}\}$ DEPT (119 MHz): δ = -9.3 (d, $^2J_{\text{PSi}} = 17.4$ Hz).

Synthesis of Compound 18. Compound 17 was generated in situ as described above (compound 10a: 28.4 mg, 0.1 mmol; $\text{PhCH}_2\text{CH}_2\text{B}(\text{C}_6\text{F}_5)_2$ (16): 45.1 mg, 0.1 mmol). Then, *n*-butylisocyanide (11 μL , 0.1 mmol, 1 equiv) was added. The solution was stirred overnight at rt, and all volatiles were removed in vacuo. The obtained solid was taken up in *n*-pentane (~5 mL) and stored at -40 °C overnight. The precipitate was collected and identified as compound 18 (50 mg, 0.06 mmol, 1 equiv). Single crystals suitable for the X-ray crystal structure analysis were obtained by slow evaporation of a saturated solution of 18 in *n*-pentane at -40 °C. Anal. Calcd for $\text{C}_{42}\text{H}_{37}\text{BF}_{10}\text{NPSi}$: C, 61.85; H, 4.57; N, 1.72. Found: C, 61.27; H, 4.74; N, 1.77. ^1H NMR (500 MHz, CD_2Cl_2 , 299 K): δ = 7.64 (m, 2H, *p*- Ph^{P}), 7.60 (m, 4H, *o*- Ph^{P}), 7.53 (m, 4H, *m*- Ph^{P}), 7.23 (m, 2H, *m*-Ph), 7.15 (m, 1H, *p*-Ph), 6.97 (m, 2H, *o*-Ph), 3.41 (m, 2H, 1-H), 2.92 (br m, 2H, $=\text{CH}_2$), 2.65 (m, 2H, $^{\text{Ph}}\text{CH}_2$), 1.41 (m, 2H, 2-H), 1.17 (m, 2H, 3-H), 0.78 (t, $^3J_{\text{HH}} = 7.4$ Hz, 3H, 4-H), 0.17 (s, $^2J_{\text{SiH}} = 6.6$ Hz, 9H, SiCH_3). $^{13}\text{C}\{^1\text{H}\}$ NMR (126 MHz): δ = 218.0 (br, $=\text{CB}$), 194.2 (br m, $\text{C}=\text{N}$), 142.5 (d, $J = 0.7$ Hz, *i*-Ph), 133.6 (d, $^2J_{\text{PC}} = 8.9$ Hz, *o*- Ph^{P}), 133.4 (d, $^4J_{\text{PC}} = 3.0$ Hz, *p*- Ph^{P}), 129.3 (d, $^3J_{\text{PC}} = 11.6$ Hz, *m*- Ph^{P}), 128.9 (*m*-Ph), 128.3 (*o*-Ph), 126.3 (*p*-Ph), 124.2 (d, $^1J_{\text{PC}} = 73.8$ Hz, *i*-

Ph^{P}), 122.3 (d, $^1J_{\text{PC}} = 47.5$ Hz, $=\text{CSi}$), 59.0 (d, $^3J_{\text{PC}} = 37.8$ Hz, C1), 44.1 (d, $^3J_{\text{PC}} = 23.7$ Hz, $=\text{CH}_2$), 35.0 ($^{\text{Ph}}\text{CH}_2$), 32.9 (d, $^4J_{\text{PC}} = 2.0$ Hz, C2), 20.9 (C3), 14.1 (C4), 1.5 (d, $^3J_{\text{PC}} = 2.0$ Hz, $^1J_{\text{SiC}} = 53.7$ Hz, SiCH_3). ^{19}F NMR (470 MHz): δ = -128.5 (br m, 2F, *o*), -160.5 (t, $^3J_{\text{FF}} = 20.2$ Hz, 1F, *p*), -165.3 (m, 2F, *m*) (C_6F_5), $[\Delta\delta^{19}\text{F}_{\text{m,p}} = 4.8]$. $^{10}\text{B}\{^1\text{H}\}$ NMR (54 MHz): δ = -14.4 (d, $^2J_{3\text{IP10B}} = 15.9$ Hz). $^{31}\text{P}\{^1\text{H}\}$ NMR (202 MHz): δ = 22.7 (q 1:1:1:1, $^2J_{3\text{IP11B}} = 50.6$ Hz). $^{29}\text{Si}\{^1\text{H}\}$ DEPT (99 MHz): δ = -9.1 (d, $^2J_{\text{PSi}} = 17.7$ Hz).

Reactions of Compounds 6 and 11a with Dihydrogen.

Synthesis of Compound 8. Compounds 3 and 6 were generated in situ as described above ($\text{HB}(\text{C}_6\text{F}_5)_2$: 69.2 mg, 0.2 mmol; dimesityl(vinyl)phosphane: 59.2 mg, 0.2 mmol; compound 5: 34.9 mg, 0.2 mmol; solvent: benzene). Then, the evacuated flask was filled with H_2 gas (1.5 bar). Subsequently, the solution was stirred overnight at an H_2 atmosphere. Then, all volatiles were removed in vacuo, and the resulting solid was washed with *n*-pentane (5 \times 5 mL). After drying in vacuo, compound 8 was isolated as a colorless solid (80 mg, 0.1 mmol, 49%). Slow diffusion of *n*-pentane into a solution of compound 8 in dichloromethane at -40 °C gave crystals that were suitable for the X-ray crystal structure analysis. mp: 146 °C. Anal. Calcd for $\text{C}_{43}\text{H}_{42}\text{BF}_{10}\text{PSi}$: C, 63.09; H, 5.17. Found: C, 62.12; H, 5.13. ^1H NMR (500 MHz, CD_2Cl_2 , 299 K): δ = 7.14 (2H), 6.99 (1H), 6.92 (2H) (Ph), 6.96 (d, $^4J_{\text{PH}} = 4.3$ Hz, 4H, *m*-mes), 6.73 (dt, $^1J_{\text{PH}} = 468.1$ Hz, $^3J_{\text{HH}} = 7.0$ Hz, PH), 3.51 (br, 1H, BH), 2.35 (m, 2H, $=\text{CH}_2$), 2.33 (m, 2H, PCH_2), 2.31 (s, 6H, *p*- CH_3^{mes}), 2.11 (s, 12H, *o*- CH_3^{mes}), -0.12 (s, $^2J_{\text{SiH}} = 6.6$ Hz, SiCH_3). $^{13}\text{C}\{^1\text{H}\}$ NMR (126 MHz): δ = 165.0 (br, $=\text{CB}$), 149.3 (*i*-Ph), 147.3 (br, $=\text{CSi}$), 146.4 (d, $^4J_{\text{PC}} = 3.0$ Hz, *p*-mes), 143.1 (d, $^2J_{\text{PC}} = 10.3$ Hz, *o*-mes), 132.2 (d, $^3J_{\text{PC}} = 11.2$ Hz, *m*-mes), 128.3, 128.2, 124.5 (Ph), 111.7 (d, $^1J_{\text{PC}} = 80.6$ Hz, *i*-mes), 31.5 (br, $=\text{CH}_2$), 25.0 (d, $^1J_{\text{PC}} = 37.8$ Hz, PCH_2), 22.1 (d, $^3J_{\text{PC}} = 7.0$ Hz, *o*- CH_3^{mes}), 21.4 (d, $^5J_{\text{PC}} = 1.2$ Hz, *p*- CH_3^{mes}), 1.3 ($^1J_{\text{SiC}} = 52.0$ Hz, SiCH_3). ^{19}F NMR (470 MHz): δ = -132.1 (*o*), -164.4 (*p*), -166.7 (*m*), $[\Delta\delta^{19}\text{F}_{\text{m,p}} = 2.3]$. ^{11}B NMR (160 MHz): δ = -19.6 (d, $^1J_{\text{BH}} \sim 85$ Hz). ^{31}P NMR (202 MHz): δ = -11.6 (d, $^1J_{\text{PH}} \sim 468$ Hz). $^{29}\text{Si}\{^1\text{H}\}$ DEPT (99 MHz): δ = -9.9.

Synthesis of Compound 13. Compounds 3 and 11a were generated in situ as described above ($\text{HB}(\text{C}_6\text{F}_5)_2$: 69.2 mg, 0.2 mmol; dimesityl(vinyl)phosphane: 59.3 mg, 0.2 mmol; compound 10a: 56.2 mg, 0.2 mmol; solvent: toluene). Then, $\text{B}(\text{C}_6\text{F}_5)_3$ (102.4 mg, 0.2 mmol, 1 equiv) in toluene (~5 mL) was added, and the evacuated flask was filled with H_2 gas (1.5 bar). After the reaction solution was stirred at rt for overnight, all volatiles were removed in vacuo. The obtained residue was washed with *n*-pentane (2 \times ca. 5 mL) and dried in vacuo to give compound 13 as a colorless solid (251 mg, 0.17 mmol, 87%). Single crystals suitable for the X-ray crystal structure analysis were obtained by diffusion of *n*-pentane into a saturated solution of 13 in dichloromethane at -40 °C. Anal. Calcd for $\text{C}_{67}\text{H}_{47}\text{B}_3\text{F}_{25}\text{P}_2\text{Si}$: C, 55.93; H, 3.29. Found: C, 56.14; H, 3.26. ^1H NMR (500 MHz, CD_2Cl_2 , 299 K): δ = 7.74 (dt, $^1J_{\text{PH}} = 475.0$ Hz, $^3J_{\text{HH}} = 7.1$ Hz, 1H, PH), 7.53 (2H), 7.39 (4H), 7.20 (4H) (Ph), 7.10 (d, $^4J_{\text{PH}} = 4.8$ Hz, *m*-mes), 3.58 (br q 1:1:1:1, $^1J_{\text{BH}} \sim 90$ Hz, 1H, BH), 3.05 (m, 2H, $=\text{CH}_2$), 2.88 (m, 2H, PCH_2), 2.36 (s, 6H, *p*- CH_3^{mes}), 2.29 (s, 12H, *o*- CH_3^{mes}), 0.06 (s, $^2J_{\text{SiH}} = 6.6$ Hz, 9H, SiCH_3). $^{13}\text{C}\{^1\text{H}\}$ NMR (126 MHz): δ = 199.7 (br, $=\text{CB}$), 147.7 (d, $^4J_{\text{PC}} = 3.0$ Hz, *p*-mes), 143.4 (d, $^2J_{\text{PC}} = 10.4$ Hz, *o*-mes), 142.4 (d, $^1J_{\text{PC}} = 27.6$ Hz, $=\text{CSi}$), 132.7 (d, $^3J_{\text{PC}} = 11.6$ Hz, *m*-mes), 132.5 (d, $^4J_{\text{PC}} = 3.0$ Hz, *p*-Ph), 132.2 (d, $^2J_{\text{PC}} = 9.3$ Hz, *o*-Ph), 129.4 (d, $^3J_{\text{PC}} = 10.6$ Hz, *m*-Ph), 125.6 (d, $^1J_{\text{PC}} = 41.6$ Hz, *i*-Ph), 109.9 (d, $^1J_{\text{PC}} = 82.3$ Hz, *i*-mes), 33.5 (d, $J_{\text{PC}} = 56.0$ Hz, $=\text{CH}_2$), 23.6 (d, $^1J_{\text{PC}} = 56.0$ Hz, PCH_2), 22.1 (d, $^3J_{\text{PC}} = 7.5$ Hz, *o*- CH_3^{mes}), 21.4 (d, $^4J_{\text{PC}} = 1.3$ Hz, *p*- CH_3^{mes}), -0.2 (d, $^3J_{\text{PC}} = 2.0$ Hz, $^1J_{\text{SiC}} = 53.1$ Hz, SiCH_3). ^{19}F NMR (470 MHz): δ = -130.5 (*o*), -156.5 (*p*), -163.6 (*m*) ($\text{B}(\text{C}_6\text{F}_5)_2$), $[\Delta\delta^{19}\text{F}_{\text{m,p}} = 7.1]$ -134.0 (*o*), -164.8 (*p*), -167.6 (*m*) ($\text{B}(\text{C}_6\text{F}_5)_3$), $[\Delta\delta^{19}\text{F} = 2.8]$. ^{11}B NMR (160 MHz): δ = -7.4 ($\text{B}(\text{C}_6\text{F}_5)_2$), -25.4 (d, $^1J_{\text{BH}} \sim 90$ Hz, $\text{B}(\text{C}_6\text{F}_5)_3$). ^{31}P NMR (202 MHz): δ = 13.1 (PPh_2), -12.2 (br d, $^1J_{\text{PH}} \sim 476$ Hz, Pmes_2). $^{29}\text{Si}\{^1\text{H}\}$ DEPT (99 MHz): δ = -10.2 (d, $^2J_{\text{PSi}} = 5.1$ Hz).

Reactions of Compounds 6 and 11a, b with Nitric Oxide.

Caution! NO is a toxic gas that must to be handled with due care.

Synthesis of Compound 9. Compounds 3 and 6 were generated in situ as described above ($\text{HB}(\text{C}_6\text{F}_5)_2$: 69.2 mg, 0.2 mmol; dimesityl-

(vinyl)phosphane: 59.2 mg, 0.2 mmol; compound **5**: 34.9 mg, 0.2 mmol; solvent: benzene). Then, the evacuated flask was filled with NO gas (1.5 bar). After 2 h stirring at rt, all volatiles were removed in vacuo. The resulting solid was washed with *n*-pentane (3 × 5 mL) to give compound **9** (102 mg, 0.12 mmol, 61%) as a slightly yellow solid. Single crystals suitable for the X-ray crystal structure analysis were obtained by diffusion of *n*-pentane into a solution of compound **9** at -40 °C. mp: 252 °C. Anal. Calcd for C₄₃H₄₀BF₁₀OPSi: C, 62.03; H, 4.84. Found: C, 61.97; H, 5.06. ¹H NMR (500 MHz, CD₂Cl₂, 299 K): δ = 7.37 (2H), 7.20 (1H), 7.04 (2H) (Ph), 6.89 (br d, ⁴J_{PH} = 4.3 Hz, 4H, *m*-mes), 2.76 (br m, 2H, PCH₂), 2.65 (br dm, ³J_{PH} = 25.8 Hz, 2H, =CH₂), 2.38 (br, 12H, *o*-CH₃^{mes}), 2.33 (m, 6H, *p*-CH₃^{mes}), -0.36 (s, ²J_{SiH} = 6.5 Hz, SiCH₃). ¹³C{¹H} NMR (126 MHz): δ = 160.1 (br, =CB), 149.0 (*i*-Ph), 144.2 (br, =CSi), 144.0 (d, ⁴J_{PC} = 2.9 Hz, *p*-mes), 142.7 (br, *o*-mes), 132.1 (d, ³J_{PC} = 12.0 Hz, *m*-mes), 128.5, 128.3, 124.8 (Ph), 123.0 (br d, ¹J_{PC} = 103.2 Hz, *i*-mes), 29.7 (d, ¹J_{PC} = 57.0 Hz, PCH₂), 29.0 (d, ²J_{PC} = 6.3 Hz, =CH₂), 22.5 (br, *o*-CH₃^{mes}), 21.0 (*p*-CH₃^{mes}), 0.2 (¹J_{SiC} = 51.8 Hz, SiCH₃). ¹⁹F NMR (470 MHz): δ = -126.7 (*o*), -159.6 (*p*), -165.9 (*m*), [Δδ¹⁹F_{*m,p*} = 6.3]. ¹¹B{¹H} NMR (160 MHz): δ = 0.0. ³¹P{¹H} NMR (202 MHz): δ = 62.4. ²⁹Si{¹H} DEPT (99 MHz): δ = -10.4.

Synthesis of Compounds 14a, b. Compound 14a. Compounds **3** and **11a** were generated in situ as described above (HB(C₆F₅)₂: 208 mg, 0.6 mmol; dimesityl(vinyl)phosphane: 178 mg, 0.6 mmol; compound **10a**: 169 mg, 0.6 mmol; solvent: benzene). Then, the evacuated flask was filled with NO gas (1.5 bar), and the solution was stirred overnight. All volatiles were removed in vacuo, and the crude product was washed with *n*-pentane (3 × 5 mL) and dried in vacuo to give compound **14a** (470 mg, 0.48 mmol, 81%) as a slightly green-blue solid. Single crystals suitable for the X-ray crystal structure analysis were obtained by slow evaporation of the solvent of a solution of **14a** in a mixture of benzene and *n*-pentane at room temperature. mp: 131 °C. Anal. Calcd for C₄₉H₄₅BF₁₀NO₂P₂Si: C, 60.63; H, 4.67; N, 1.44. Found: C, 60.28; H, 5.03; N, 1.33.

Compound 14b. Compound **11b** (286 mg, 0.3 mmol, 1 equiv) was dissolved in benzene (~2 mL), and the evacuated flask was filled with NO gas (1.5 bar). The reaction solution was stirred for overnight, and then, all volatiles were removed in vacuo. The resulting solid was washed with *n*-pentane (3 × 5 mL) and dried in vacuo to give compound **14b** (260 mg, 0.26 mmol, 87%) as a green solid. Single crystals suitable for the X-ray crystal structure analysis were obtained by diffusion of *n*-pentane into a saturated solution of **14b** at -40 °C. Anal. Calcd for C₅₁H₄₉BF₁₀NO₂P₂Si: C, 61.33; H, 4.94; N, 1.08. Found: C, 61.36; H, 5.11; N, 0.95.

Synthesis of Compounds 25a, b. General Procedure. Compound **11a** (555 mg, 0.6 mmol, 1 equiv; **11b**: 270 mg, 0.28 mmol, 1 equiv) was dissolved in toluene (~5 mL), and the solution was cooled to -78 °C. At this temperature, NO (30 mL, 1.3 mmol, 2.2 equiv; **11b**: 14.0 mL, 2.2 equiv) was added slowly via a syringe directly into the solution within ~2 min. After that, the resulting solution was stirred for 30 min at -78 °C, warmed to rt, and stirred at rt for 1 h (**25b**: the solution was stirred at rt for overnight). The reaction process was controlled by ³¹P NMR experiments to indicate complete conversion to **25a** (**25b**). Then, all volatiles were removed in vacuo, *n*-pentane (~10 mL) was added to the residue, and the obtained suspension was sonicated for 5 min. The supernatant was taken off, and the solid was dried in vacuo to give compound **25a** (460 mg, 0.49 mmol, 82%; **25b**: 180 mg, 0.24 mmol, 85%) as a colorless solid. Single crystals suitable for the X-ray crystal structure analysis were obtained by diffusion of *n*-pentane into a solution of compound **25a** in dichloromethane at -40 °C. Single crystals suitable for the X-ray crystal structure analysis of compound **25b** were obtained by slow evaporation of a saturated solution of **25b** in C₆D₆ at rt.

Compound 25a. Decomp: 171 °C. Anal. Calcd for C₄₉H₄₅BF₁₀NOP₂Si: C, 62.56; H, 4.82. Found: C, 63.09; H, 5.20. ¹H NMR (600 MHz, tol-*d*₈, 299 K): δ = 7.20 (4H), 6.87 (2H), 6.81 (4H) (Ph), 6.51 (d, ⁴J_{PH} = 3.1 Hz, 4H, *m*-mes), 3.35 (m, 2H, =CH₂), 2.53 (m, 2H, PCH₂), 2.31 (s, 12H, *o*-CH₃^{mes}), 1.95 (s, 6H, *p*-CH₃^{mes}), 0.09 (s, ²J_{SiH} = 6.6 Hz, 9H, SiCH₃). ¹³C{¹H} NMR (151 MHz): δ = 207.7 (br, =CB), 141.4 (br d, ²J_{PC} = 9.5 Hz, *o*-mes), 140.6 (*p*-mes),

137.8 (d, ¹J_{PC} = 24.8 Hz, =CSi)¹ 132.0 (d, ²J_{PC} = 9.8 Hz, *o*-Ph), 131.4 (m, *m*-mes), 131.4 (m, *p*-Ph), 130.7 (br d, ¹J_{PC} ~ 90 Hz, *i*-mes), 128.8 (*m*-Ph), 127.7 (*i*-Ph), 35.1 (d, ¹J_{PC} = 62.0 Hz, PCH₂), 33.3 (d, ¹J_{PC} = 51.3 Hz, =CH₂), 22.7 (br d, ³J_{PC} = 3.2 Hz, *o*-CH₃^{mes}), 20.7 (br, *p*-CH₃^{mes}), 0.2 (br, SiCH₃). ¹⁹F NMR (564 MHz): δ = -129.5 (*o*), -157.7 (*p*), -163.8 (*m*), [Δδ¹⁹F_{*m,p*} = 6.1]. ¹⁰B{¹H} NMR (64 MHz): δ = -6.5. ³¹P{¹H} NMR (243 MHz): δ = 37.4 (Pmes₂), 13.4 (PPh₂). ²⁹Si{¹H} DEPT (119 MHz): δ = -10.8.

Compound 25b. Mp: 203 °C. Anal. Calcd for C₅₁H₄₉BF₁₀NOP₂Si: C, 63.23; H, 5.10. Found: C, 63.53; H, 5.27. ¹H NMR (500 MHz, tol-*d*₈, 299 K): δ = 7.17 (2H), 6.85 (2H), 6.71 (2H), 6.69 (2H) (^otol), 6.55 (d, ⁴J_{PH} = 3.2 Hz, 4H, *m*-mes), 3.29 (br, 2H, =CH₂), 2.66 (m, 2H, PCH₂), 2.39 (s, 12H, *o*-CH₃^{mes}), 2.20 (br, 6H, *o*-CH₃^{o-tol}), 1.94 (s, 6H, *p*-CH₃^{mes}), 0.14 (s, ²J_{SiH} = 6.6 Hz, 9H, SiCH₃). ¹³C{¹H} NMR (126 MHz): δ = 204.5 (br, =CB), 142.1 (d, ²J_{PC} = 11.4 Hz, *o*-tol), 141.4 (d, ²J_{PC} = 10.3 Hz, *o*-mes), 140.7 (*p*-mes), 139.1 (m, =CSi), 133.9 (d, ²J_{PC} = 5.6 Hz, *o*'-tol), 131.5 (m, *m,p*-tol), 131.5 (m, *m*-mes), 130.8 (br d, ¹J_{PC} ~ 90 Hz, *i*-mes), 126.6 (*i*-tol), 126.1 (d, ³J_{PC} = 8.3 Hz, *m*'-tol), 34.8 (d, ¹J_{PC} = 63.6 Hz, PCH₂), 32.9 (d, ¹J_{PC} = 51.4 Hz, =CH₂), 22.9 (d, ³J_{PC} = 3.9 Hz, *o*-CH₃^{mes}), 22.1 (br d, ³J_{PC} = 5.8 Hz, *o*-CH₃^{o-tol}), 20.8 (d, ⁵J_{PC} = 1.2 Hz, *p*-CH₃^{mes}), 0.1 (br, SiCH₃). ¹⁹F NMR (470 MHz): δ = -128.6 (*o*), -157.4 (*p*), -163.6 (*m*), [Δδ¹⁹F_{*m,p*} = 6.2]. ³¹P{¹H} NMR (202 MHz): δ = 37.4 (Pmes₂), 18.3 (P^otol₂). ¹⁰B{¹H} NMR (54 MHz): δ = -1.6. ²⁹Si{¹H} DEPT (99 MHz): δ = -10.5 (d, ²J_{Psi} = 7.5 Hz).

Synthesis of Compounds 15a, b. Compound 15a. Compound **25a** (47.0 mg, 0.05 mmol, 1 equiv) was dissolved in toluene (~2 mL), NO gas (1.5 bar) was added to the evacuated flask, and it was stirred at rt for overnight. At the next day, the gas phase was removed in vacuo, and 1,4-cyclohexadiene (5 μL, 0.05 mmol, 1 equiv) was added. After stirring for 2 h at rt, all volatiles were removed in vacuo. The residue was washed with *n*-pentane (1 × ~5 mL) and dried in vacuo to give compound **15a** (36.0 mg, 0.04 mmol, 74%) as a colorless solid. Single crystals suitable for X-ray crystal structure analysis were obtained from a saturated solution of compound **15a** (stored in a flame-sealed NMR tube) in CD₂Cl₂ after 3 days at rt. Decomp: 239 °C. Anal. Calcd for C₄₉H₄₆BF₁₀NO₂P₂Si: C, 60.57; H, 4.77; N, 1.44. Found: C, 60.58; H, 4.88; N, 1.16. ¹H NMR (500 MHz, CD₂Cl₂, 299 K): δ = 7.72 (4H), 7.68 (2H), 7.55 (4H) (Ph), 6.78 (d, ⁴J_{PH} = 3.2 Hz, 4H, *m*-mes), 4.31 (d, ³J_{PH} = 5.1 Hz, NOH), 2.77 (m, 2H, =CH₂), 2.42 (m, 2H, PCH₂), 2.24 (s, 6H, *p*-CH₃^{mes}), 2.21 (s, 12H, *o*-CH₃^{mes}), 0.06 (s, 9H, ²J_{SiH} = 6.5 Hz, SiCH₃). ¹³C{¹H} NMR (126 MHz): δ = 207.8 (br, =CB), 141.2 (d, ²J_{PC} = 9.9 Hz, *o*-mes), 141.1 (d, ⁴J_{PC} = 2.3 Hz, *p*-mes), 134.12 (d, ²J_{PC} = 10.1 Hz, *o*-Ph), 134.08 (d, ⁴J_{PC} = 2.8 Hz, *p*-Ph), 131.3 (d, ³J_{PC} = 10.9 Hz, *m*-mes), 130.1 (d, ¹J_{PC} = 92.8 Hz, *i*-mes), 129.2 (d, ³J_{PC} = 12.1 Hz, *m*-Ph), 124.3 (d, ¹J_{PC} = 92.5 Hz, *i*-Ph), 122.7 (d, ¹J_{PC} = 56.6 Hz, =CSi), 34.9 (d, ¹J_{PC} = 65.7 Hz, PCH₂), 31.8 (d, ¹J_{PC} = 26.1 Hz, =CH₂), 22.7 (d, ³J_{PC} = 4.0 Hz, *o*-CH₃^{mes}), 20.9 (d, ⁵J_{PC} = 1.1 Hz, *p*-CH₃^{mes}), 0.8 (d, ³J_{PC} = 2.7 Hz, ¹J_{SiC} = 53.6 Hz, SiCH₃). ¹⁹F NMR (470 MHz): δ = -130.8 (*o*), -160.4 (*p*), -164.8 (*m*), [Δδ¹⁹F_{*m,p*} = 4.4]. ¹⁰B{¹H} NMR (54 MHz): δ = -5.6. ³¹P{¹H} NMR (202 MHz): δ = 52.0 (PPh₂), 38.9 (d, ⁵J_{PP} = 1.9 Hz, Pmes₂). ²⁹Si{¹H} DEPT (99 MHz): δ = -9.5 (d, ²J_{Psi} = 24.2 Hz).

Compound 15b. Compound **14b** (100 mg, 0.1 mmol, 1 equiv) was dissolved in toluene (~3 mL), and 1,4-cyclohexadiene (10 μL, 0.11 mmol, 1.1 equiv) was added at rt. The resulting solution was stirred for 2 h at rt, all volatiles were removed in vacuo, and *n*-pentane (~5 mL) was added to the residue. The solvent was immediately removed again in vacuo, and the crude product was washed with *n*-pentane (~5 mL) to give **15b** (70.0 mg, 0.9 mmol, 89%) as a colorless solid. Single crystals suitable for X-ray crystal structure analysis were obtained by slow evaporation of a saturated solution of **15b** in CD₂Cl₂ at rt. Decomp: 231 °C. Anal. Calcd for C₅₁H₅₀BF₁₀NO₂P₂Si: C, 61.27; H, 5.04; N, 1.08. Found: C, 60.76; H, 5.01; N, 1.17. ¹H NMR (600 MHz, CD₂Cl₂, 299 K): δ = 7.67 (*o*'), 7.50 (*p*'), 7.33 (*m*'), 7.32 (*m*) (each m, each 1H, ^otol²), 7.56 (*p*'), 7.42 (*o*'), 7.39 (*m*'), 7.24 (*m*') (each m, each 1H, ^otol¹), 6.80 (d, ⁴J_{PH} = 3.0 Hz, 4H, *m*-mes^{1,2}), 4.57 (d, ³J_{PH} = 5.2 Hz, NOH), 3.11, 3.02 (each m, each 1H, =CH₂), 2.62 (s, 3H, *o*-CH₃^{o-tol1}), 2.43 (s, 3H, *o*-CH₃^{o-tol2}), 2.25 (s, 3H, *p*-CH₃^{mes2}), 2.24 (s,

3H, *p*-CH₃^{mes1}), 2.20 (s, 6H, *o*-CH₃^{mes1}), 2.18 (m, 2H, PCH₂), 2.16 (s, 6H, *o*-CH₃^{mes2}), 0.07 (s, ²J_{SiH} = 6.6 Hz, 9H, SiCH₃). ¹³C{¹H} NMR (151 MHz): δ = 207.5 (br, =CB), 145.4 (d, ²J_{PC} = 8.9 Hz, *o*), 137.1 (d, ²J_{PC} = 14.9 Hz, *o'*), 134.4 (d, ⁴J_{PC} = 3.0 Hz, *p*), 133.1 (d, ³J_{PC} = 10.8 Hz, *m*), 126.4 (d, ³J_{PC} = 13.7 Hz, *m'*), 122.5 (d, ¹J_{PC} = 92.3 Hz, *i*) (^otol¹), 143.7 (d, ²J_{PC} = 6.2 Hz, *o*), 134.7 (d, ²J_{PC} = 14.3 Hz, *o'*), 133.3 (d, ⁴J_{PC} = 2.7 Hz, *p*), 132.7 (d, ³J_{PC} = 10.3 Hz, *m*), 125.8 (d, ³J_{PC} = 12.9 Hz, *m'*), 124.6 (d, ¹J_{PC} = 81.9 Hz, *i*) (^otol²), 141.22, 141.17 (each d, ⁴J_{PC} = 2.7 Hz, *p*-mes^{1,2}), 141.08 (d, ²J_{PC} = 9.9 Hz, *o*-mes²), 141.04 (d, ²J_{PC} = 9.9 Hz, *o*-mes¹), 131.40, 131.39 (each d, ³J_{PC} = 11.0 Hz, *m*-mes^{1,2}), 130.4 (d, ¹J_{PC} = 93.5 Hz, *i*-mes¹), 129.8 (d, ¹J_{PC} = 92.9 Hz, *i*-mes²), 123.0 (d, ¹J_{PC} = 56.9 Hz, =CSi), 36.7 (d, ¹J_{PC} = 62.9 Hz, PCH₂), 31.1 (d, ¹J_{PC} = 24.5 Hz, =CH₂), 24.3 (d, ³J_{PC} = 1.9 Hz, *o*-CH₃^{o-tol2}), 22.9 (d, ³J_{PC} = 4.0 Hz, *o*-CH₃^{mes1}), 22.7 (d, ³J_{PC} = 4.0 Hz, *o*-CH₃^{mes2}), 21.0, 21.0 (each d, ⁴J_{PC} = 1.0 Hz, *p*-CH₃^{mes1,2}), 20.5 (m, *o*-CH₃^{o-tol1}), 0.9 (d, ³J_{PC} = 2.8 Hz, ¹J_{SiC} = 53.1 Hz, SiCH₃). ³¹P{¹H} NMR (243 MHz): δ = 53.3 (P(*o*-tol)), 38.6 (d, ⁵J_{PP} = 1.5 Hz, Pmes). ¹⁰B{¹H} NMR (64 MHz): δ = -5.3. ²⁹Si{¹H} DEPT (119 MHz): δ = -9.3 (d, ²J_{PSi} = 23.6 Hz). ¹⁹F NMR (564 MHz): δ = -129.3 (br m, 2F, *o*), -161.0 (t, ³J_{FF} = 20.0 Hz, 1F, *p*), -165.0 (m, 2F, *m*) (C₆F₅), [Δδ¹⁹F_{m,p} = 4.0] -132.2 (br m, 2F, *o*), -159.9 (t, ³J_{FF} = 20.4 Hz, 1F, *p*), -163.7 (m, 2F, *m*) (C₆F₅), [Δδ¹⁹F_{m,p} = 3.8].

Synthesis of Compound 28a. Compounds **3** and **11a** were generated in situ as described above (HB(C₆F₅)₂): 138 mg, 0.4 mmol; dimesityl(vinyl)phosphane: 119 mg, 0.4 mmol; compound **10a**: 113 mg, 0.4 mmol; solvent: toluene). Then, S₈ (3.2 mg, 0.01 mmol, 0.13 equiv) was added to the solution, and the resulting solution was stirred for 2 days at rt. All volatiles were removed in vacuo, and the resulting solid was washed with *n*-pentane (4 × ~5 mL) and dried in vacuo to give compound **28a** (280 mg, 0.29 mmol, 73%) as a colorless solid. Single crystals suitable for the X-ray crystal structure analysis were obtained by slow diffusion of *n*-pentane into a solution of **28a** in dichloromethane at -40 °C. mp: 254 °C. Anal. Calcd for C₄₉H₄₅BF₁₀P₂SSi: C, 61.51; H, 4.74. Found: C, 62.48; H, 4.79. ¹H NMR (500 MHz, CD₂Cl₂, 299 K): δ = 7.48 (2H), 7.36 (4H), 7.24 (4H) (Ph), 6.81 (d, ⁴J_{PH} = 4.0 Hz, 4H, *m*-mes), 3.06 (m, 2H, =CH₂), 2.63 (m, 2H, PCH₂), 2.24 (s, 6H, *p*-CH₃^{mes}), 2.24 (s, 12H, *o*-CH₃^{mes}), 0.10 (s, ²J_{SiH} = 6.6 Hz, 9H, SiCH₃). ¹³C{¹H} NMR (126 MHz): δ = 206.7 (br, =CB), 140.8 (d, ⁴J_{PC} = 2.7 Hz, *p*-mes), 140.3 (d, ²J_{PC} = 9.8 Hz, *o*-mes), 138.7 (d, ¹J_{PC} = 27.6 Hz, =CSi), 132.3 (d, ²J_{PC} = 9.2 Hz, *o*-Ph), 132.1 (d, ³J_{PC} = 10.6 Hz, *m*-mes), 131.9 (d, ⁴J_{PC} = 3.0 Hz, *p*-Ph), 130.3 (d, ¹J_{PC} = 76.2 Hz, *i*-mes), 129.1 (d, ³J_{PC} = 10.4 Hz, *m*-Ph), 127.1 (d, ¹J_{PC} = 39.2 Hz, *i*-Ph), 39.0 (d, ¹J_{PC} = 52.1 Hz, PCH₂), 33.8 (d, ¹J_{PC} = 53.6 Hz, =CH₂), 23.3 (d, ³J_{PC} = 4.9 Hz, *o*-CH₃^{mes}), 20.9 (d, ⁵J_{PC} = 1.5 Hz, *p*-CH₃^{mes}), -0.1 (d, ²J_{PC} = 2.3 Hz, ¹J_{SiC} = 52.9 Hz, SiCH₃). ¹⁹F NMR (470 MHz): δ = -129.9 (*o*), -158.3 (*p*), -164.7 (*m*), [Δδ¹⁹F_{m,p} = 6.4]. ¹⁰B{¹H} NMR (54 MHz): δ = -7.0. ³¹P{¹H} NMR (202 MHz): δ = 42.8 (d, ⁵J_{PP} = 3.6 Hz, Pmes₂), 13.6 (PPh₂). ²⁹Si{¹H} DEPT (99 MHz): δ = -10.8 (d, ²J_{PSi} = 5.8 Hz).

■ ASSOCIATED CONTENT

● Supporting Information

Detailed description of experiments, characterization of all new compounds, and crystal structure data as CIF files. This material is available free of charge via the Internet at <http://pubs.acs.org>.

■ AUTHOR INFORMATION

Corresponding Authors

eckerth@uni-muenster.de
thwarren@purdue.edu
grimme@thch.uni-bonn.de
erker@uni-muenster.de

Notes

The authors declare no competing financial interest.

B.S. is member of the Center for Multiscale Theory and Computation (CMTC), Universität Münster, Corrensstr. 40, 48149 Münster, Germany.

■ ACKNOWLEDGMENTS

Financial support from SusChemSys, the European Research Council, and the Deutsche Forschungsgemeinschaft (DFG) is gratefully acknowledged. The project "Sustainable Chemical Synthesis (SusChemSys)" is cofinanced by the European Regional Development Fund (ERDF) and the state of North Rhine-Westphalia, Germany, under the Operational Programme "Regional Competitiveness and Employment" 2007–2013. T.H.W. thanks the U.S. National Science Foundation for an EPR spectrometer (CHE-0840453) as well as the Petroleum Research Fund (51971-ND3).

■ REFERENCES

- (1) Kehr, G.; Schwendemann, S.; Erker, G. *Top. Curr. Chem.* **2013**, *332*, 45.
- (2) Ekkert, O.; Miera, G. G.; Wiegand, T.; Eckert, H.; Schirmer, B.; Peterson, J. L.; Daniliuc, C. G.; Fröhlich, R.; Grimme, S.; Kehr, G.; Erker, G. *Chem. Sci.* **2013**, *4*, 2657.
- (3) (a) Ekkert, O.; Kehr, G.; Fröhlich, R.; Erker, G. *J. Am. Chem. Soc.* **2011**, *133*, 4610. (b) Ekkert, O.; Kehr, G.; Fröhlich, R.; Erker, G. *Chem. Commun.* **2013**, *47*, 10482. (c) See for a comparison: Sajid, M.; Lawzer, A.; Dong, W.; Rosorius, C.; Sander, W.; Schirmer, B.; Grimme, S.; Daniliuc, C. G.; Kehr, G.; Erker, G. *J. Am. Chem. Soc.* **2013**, *135*, 18567.
- (4) (a) Dewar, M. *Bull. Soc. Chim. Fr.* **1951**, *18*, C79. (b) Chatt, J.; Duncanson, L. A. *J. Chem. Soc.* **1953**, 2939. (c) Chatt, J.; Duncanson, L. A.; Venanzi, L. M. *J. Chem. Soc.* **1955**, 4456.
- (5) Spies, P.; Erker, G.; Kehr, G.; Bergander, K.; Fröhlich, R.; Grimme, S.; Stephan, D. W. *Chem. Commun.* **2007**, 5072.
- (6) (a) Warren, T. H.; Erker, G. *Top. Curr. Chem.* **2013**, *334*, 219. See also: (b) Otten, E.; Neu, R. C.; Stephan, D. W. *J. Am. Chem. Soc.* **2009**, *131*, 9918–9919. (c) Cardenas, A. J. P.; Culotta, B. J.; Warren, T. H.; Grimme, S.; Stute, A.; Fröhlich, R.; Kehr, G.; Erker, G. *Angew. Chem., Int. Ed.* **2011**, *50*, 7567. (d) Sajid, M.; Stute, A.; Cardenas, A. J. P.; Culotta, B. J.; Hepperle, J. A. M.; Warren, T. H.; Schirmer, B.; Grimme, S.; Studer, A.; Daniliuc, C. G.; Fröhlich, R.; Petersen, J. L.; Kehr, G.; Erker, G. *J. Am. Chem. Soc.* **2012**, *134*, 10156. (e) Sajid, M.; Kehr, G.; Wiegand, T.; Eckert, H.; Schwickert, C.; Pöttgen, R.; Cardenas, A. J. P.; Warren, T. H.; Fröhlich, R.; Daniliuc, C. G.; Erker, G. *J. Am. Chem. Soc.* **2013**, *135*, 8882. (f) Pereira, J. C. M.; Sajid, M.; Kehr, G.; Wright, A. M.; Schirmer, B.; Qu, Z.-W.; Grimme, S.; Erker, G.; Ford, P. C. *J. Am. Chem. Soc.* **2014**, *136*, 513–519.
- (7) (a) Wrackmeyer, B. *Coord. Chem. Rev.* **1995**, *145*, 125. (b) Wrackmeyer, B. *Heteroat. Chem.* **2006**, *17*, 188 (see also references cited herein).
- (8) Kehr, G.; Erker, G. *Chem. Commun.* **2012**, *48*, 1839 (see also references cited herein).
- (9) (a) Chen, C.; Eweiner, F.; Wibbeling, B.; Fröhlich, R.; Senda, S.; Ohki, Y.; Tatsumi, K.; Grimme, S.; Kehr, G.; Erker, G. *Chem.—Asian J.* **2010**, *5*, 2199. (b) Chen, C.; Voss, T.; Fröhlich, R.; Kehr, G.; Erker, G. *Org. Lett.* **2010**, *13*, 62.
- (10) Chen, C.; Kehr, G.; Fröhlich, R.; Erker, G. *J. Am. Chem. Soc.* **2010**, *132*, 13594.
- (11) (a) Dierker, G.; Ugolotti, J.; Kehr, G.; Fröhlich, R.; Erker, G. *Adv. Synth. Catal.* **2009**, *351*, 1080. (b) Chen, C.; Fröhlich, R.; Kehr, G.; Erker, G. *Chem. Commun.* **2010**, *46*, 3580. (c) Möbus, J.; Bonnin, Q.; Ueda, K.; Fröhlich, R.; Itami, K.; Kehr, G.; Erker, G. *Angew. Chem., Int. Ed.* **2012**, *51*, 1954. (d) Liedtke, R.; Harhausen, M.; Fröhlich, R.; Kehr, G.; Erker, G. *Org. Lett.* **2012**, *14*, 1448.
- (12) Jiang, C.; Blacque, O.; Berke, H. *Organometallics* **2010**, *29*, 125. (b) Fan, C.; Piers, W. E.; Parvez, M.; McDonald, R. *Organometallics* **2010**, *29*, 5132.

(13) Mömning, C. M.; Kehr, G.; Wibbeling, B.; Fröhlich, R.; Erker, G. *Dalton Trans.* **2010**, 39, 7556.

(14) See for a formal comparison: Jahnke, E.; Tykwinski, R. R. *Chem. Commun.* **2010**, 46, 3235.

(15) See for a comparison: (a) Köster, R.; Seidel, G.; Süß, J.; Wrackmeyer, B. *Chem. Ber.* **1993**, 126, 1107. (b) Wrackmeyer, B.; Tok, O. L.; Klimkina, E. V.; Milius, W. *Eur. J. Inorg. Chem.* **2010**, 2276. (c) Wrackmeyer, B.; Tok, O. L. *Comprehensive Heterocyclic Chemistry III*; Katritzky, A. R., Ramsden, C. A., Scriven, E. F. V., Taylor, R. J. K., Eds.; Elsevier: Oxford, U.K., 2008; Ch 3.17, p 1181, and references cited herein.

(16) (a) Stephan, D. W.; Erker, G. *Angew. Chem., Int. Ed.* **2010**, 49, 46. (b) Stephan, D. W.; Erker, G. *Top. Curr. Chem.* **2013**, 332, 85.

(17) (a) Longhi, R.; Ragsdale, R. O.; Drago, R. S. *Inorg. Chem.* **1962**, 1, 768. (b) Lim, M. D.; Lorkovic, I. M.; Ford, P. C. *Inorg. Chem.* **2002**, 41, 1026. (c) Zhao, Y.-L.; Flora, J. W.; Thweatt, W. D.; Garrison, S. L.; Gonzalez, C.; Houk, K. N.; Marquez, M. *Inorg. Chem.* **2009**, 48, 1223.

(18) Ekkert, O.; Kehr, G.; Daniliuc, C. G.; Fröhlich, R.; Wibbeling, B.; Petersen, J. L.; Erker, G. *Z. Anorg. Allg. Chem.* **2013**, 639, 2455.

(19) (a) Welch, G. C.; Stephan, D. W. *J. Am. Chem. Soc.* **2007**, 129, 1880. (b) Otten, E.; Neu, R. C.; Stephan, D. W. *J. Am. Chem. Soc.* **2009**, 131, 9918. (c) Neu, R. C.; Otten, E.; Lough, A.; Stephan, D. W. *Chem. Sci.* **2011**, 2, 170. (d) Liedtke, R.; Fröhlich, R.; Kehr, G.; Erker, G. *Organometallics* **2011**, 30, 5222.

(20) NO: (a) Nichols, N. L.; Hause, C. D.; Noble, R. H. *J. Chem. Phys.* **1955**, 23, 57. TEMPO: (b) Talsi, E. P.; Semikolenova, N. V.; Panchenko, V. N.; Sobolev, A. P.; Babushkin, D. E.; Shubin, A. A.; Zakharov, V. A. *J. Mol. Catal. A* **1999**, 139, 131. (c) Yonekuta, Y.; Oyaizu, K.; Nishide, H. *Chem. Lett.* **2007**, 36, 866.

(21) Tebben, L.; Studer, A. *Angew. Chem., Int. Ed.* **2011**, 50, 5034.

(22) Wiegand, T.; Eckert, H.; Ekkert, O.; Fröhlich, R.; Kehr, G.; Erker, G.; Grimme, S. *J. Am. Chem. Soc.* **2012**, 134, 4236.

(23) Parks, D. J.; Piers, W. E.; Yap, G. P. A. *Organometallics* **1998**, 17, 5492.

(24) Parks, D. J.; Spence, R. E. v. H.; Piers, W. E. *Angew. Chem., Int. Ed.* **1995**, 34, 809.

(25) (a) Beckett, M. A.; Brassington, D. S.; Light, M. E.; Hursthouse, M. B. *J. Chem. Soc., Dalton Trans.* **2001**, 1768. (b) Britovsek, G. J. P.; Ugolotti, J.; White, A. J. P. *Organometallics* **2005**, 24, 1685. (c) Hill, M.; Herrmann, C.; Spies, P.; Kehr, G.; Bergander, K.; Fröhlich, R.; Erker, G. In *Activating Unreactive Substrates: The Role of Secondary Interactions*; Bolm, C., Hahn, F. E., Eds.; Wiley-VCH: Weinheim, Germany, 2009; p 209. (d) Frömel, S.; Fröhlich, F.; Daniliuc, C. G.; Kehr, G.; Erker, G. *Eur. J. Inorg. Chem.* **2010**, 3774. (e) Porcel, S.; Saffon, N.; Bouhadir, G.; Maron, L.; Bourissou, D. *Angew. Chem., Int. Ed.* **2010**, 49, 6186. (f) Dureen, M. A.; Brown, C. C.; Stephan, D. W. *Organometallics* **2010**, 29, 6422. (g) Morgan, M. M.; Marwitz, A. J. V.; Piers, W. E.; Parvez, M. *Organometallics* **2013**, 32, 317. (h) Mohr, J.; Durmaz, M.; Irran, E.; Oestreich, M. *Organometallics* **2014**, 33, 1108.

(26) Structures were calculated at the B2PLYP-D3/def2-TZVP level of theory, thermal corrections with TPSS-D3/def2-TZVP and high convergence criteria (see the Supporting Information for details), solvent corrections with COSMO-RS; the general accuracy of the resulting $\Delta G_{\text{solution}}$ data is assumed to be about 1–2 kcal mol⁻¹. (a) Grimme, S. *J. Chem. Phys.* **2006**, 124, 034108. (b) Grimme, S.; Antony, J.; Ehrlich, S.; Krieg, H. *J. Chem. Phys.* **2010**, 132, 154104. (c) Grimme, S.; Ehrlich, S.; Goerigk, L. *J. Comput. Chem.* **2011**, 32, 1456. (d) Weigend, F.; Ahlrichs, R. *Phys. Chem. Chem. Phys.* **2005**, 7, 3297. (e) Eckert, F.; Klamt, A. *COSMOtherm*, Version C2.1, release 01.11; COSMOlogic GmbH & Co. KG: Leverkusen, Germany, 2010. (f) Ahlrichs, R. et al. *TURBOMOLE*, versions 6.3 and 6.4; Universität Karlsruhe: Karlsruhe, Germany, **2011** and **2012**; see www.turbomole.com.

(27) (a) Yu, J.; Kehr, G.; Daniliuc, C. G.; Erker, G. *Eur. J. Inorg. Chem.* **2013**, 3312. (b) Möbus, J.; Kehr, G.; Daniliuc, C. G.; Fröhlich, R.; Erker, G. *Dalton Trans.* **2013**, 43, 632.